J|A|C|S
ARTICLES
Published on Web 03/14/2006

Ultrafast Charge Separation in a Photoreactive Rhenium-Appended Porphyrin Assembly Monitored by Picosecond Transient Infrared Spectroscopy

Anders Gabrielsson,[†] František Hartl,[‡] Hong Zhang,[‡] John R. Lindsay Smith,[†] Michael Towrie,[§] Antonín Vlček, Jr.,[||] and Robin N. Perutz*,[†]

Contribution from the Department of Chemistry, University of York, York, YO10 5DD, United Kingdom, Van't Hoff Institute for Molecular Sciences, Molecular Photonic Materials, University of Amsterdam, Nieuwe Achtergracht 166, Amsterdam, NL-1018 WV, The Netherlands, Rutherford Appleton Laboratory, Central Laser Facility, CCLRC, Didcot, Oxon, OX11 0QX, United Kingdom, and Department of Chemistry, Queen Mary, University of London, London, E1 4NS, United Kingdom

Received June 16, 2005; E-mail: rnp1@york.ac.uk

Abstract: Rhenium(bipyridine)(tricarbonyl)(picoline) units have been linked covalently to tetraphenylmetalloporphyrins of magnesium and zinc via an amide bond between the bipyridine and one phenyl substituent of the porphyrin. The resulting complexes, abbreviated as **[Re(CO)$_3$(Pic)Bpy-MgTPP][OTf]** and **[Re(CO)$_3$-(Pic)Bpy-ZnTPP][OTf]**, exhibit no signs of electronic interaction between the Re(CO)$_3$(bpy) units and the metalloporphyrin units in their ground states. However, emission spectroscopy reveals solvent-dependent quenching of porphyrin emission on irradiation into the long-wavelength absorption bands localized on the porphyrin. The characteristics of the excited states have been probed by picosecond time-resolved absorption (TRVIS) spectroscopy and time-resolved infrared (TRIR) spectroscopy in nitrile solvents. The presence of the charge-separated state involving electron transfer from MgTPP or ZnTPP to Re(bpy) is signaled in the TRIR spectra by a low-frequency shift in the ν(CO) bands of the Re(CO)$_3$ moiety similar to that observed by spectroelectrochemical reduction. Long-wavelength excitation of **[Re(CO)$_3$(Pic)Bpy-MTPP][OTf]** results in characteristic TRVIS spectra of the S_1 state of the porphyrin that decay with a time constant of 17 ps (M = Mg) or 24 ps (M = Zn). The IR bands of the CS state appear on a time scale of less than 1 ps (Mg) or ca. 5 ps (Zn) and decay giving way to a vibrationally excited (i.e., hot) ground state via back electron transfer. The IR bands of the precursors recover with a time constant of 35 ps (Mg) or 55 ps (Zn). The short lifetimes of the charge-transfer states carry implications for the mechanism of reaction in the presence of triethylamine.

Introduction

Research into donor−bridge−acceptor assemblies capable of photoinduced electron transfer has proliferated in recent years.[1−6] Particular interest has been devoted to porphyrin-containing supramolecules because of their resemblance to nature's choice of chromophores, their tunability, and low reorganization energy upon reduction or oxidation.[7−9] There are now many different porphyrins linked to organic electron donors and/or acceptors, through covalent, coordination, or hydrogen bonds as well as mechanically interlocked systems.[4,9−19] Photoinduced charge transfer is typically studied by time-resolved spectroscopy. Vibrational spectroscopic methods can provide an unequivocal demonstration of changes in charge distribution and are central to the current study. Therien's demonstration by time-resolved

[†] University of York.
[‡] University of Amsterdam.
[§] Rutherford Appleton Laboratory.
[||] Queen Mary, University of London.

(1) Balzani, V.; Scandola, F. *Supramolecular photochemistry*; Ellis Horwood: Chichester, 1991.
(2) Gust, D.; Moore, T. A.; Moore, A. L. *Acc. Chem. Res.* **2001**, *34*, 40−48.
(3) Meyer, T. J. *Prog. Inorg. Chem.* **1983**, *30*, 389−440.
(4) Ward, M. D. *Chem. Soc. Rev.* **1997**, *26*, 365−375.
(5) Wasielewski, M. R. *Chem. Rev.* **1992**, *92*, 435−461.
(6) Balaban, T. S. *Light-harvesting nanostructures*; American Scientific Publishers: 2004; Vol. 4.
(7) Kalyanasundaram, K. *Photochemistry of Polypyridine and Porphyrin Complexes*; Academic Press Limited: San Diego, 1992.
(8) Kalyanasundaram, K., Grätzel, M., Eds. *Photosenitization and Photocatalysis Using Inorganic and Organometallic Compounds*; Kluwer Academic Press: Dordrecht, 1993.
(9) Kadish, K. M., Smith, K. M., Guilard, R., Eds. *The Porphyrin Handbook*; Academic Press: San Diego, 2000; Vol. 8.
(10) Sakamoto, M.; Ueno, A.; Mihara, H. *Chem.—Eur. J.* **2001**, *7*, 2449−2458.
(11) Luo, C.; Guldi, D. M.; Imahori, H.; Tamaki, K.; Sakata, K. *J. Am. Chem. Soc.* **2000**, *122*, 6535−6551.
(12) Myles, A. J.; Branda, N. R. *J. Am. Chem. Soc.* **2001**, *123*, 177−178.
(13) Osuka, A.; Yoneshima, R.; Shiratori, H.; Okada, T.; Taniguchi, S.; Mataga, N. *Chem. Commun.* **1998**, 1567−1568.
(14) Linke, M.; Chambron, S. C.; Heitz, V.; Sauvage, S. P.; Encinas, S.; Barigelletti, F.; Flamigni, L. *J. Am. Chem. Soc.* **2000**, *122*, 11834−11844.
(15) Harriman, A.; Sauvage, J. P. *Chem. Soc. Rev.* **1996**, *25*, 41−48.
(16) Dixon, I. M.; Collin, J. P.; Sauvage, J. P.; Barigelletti, F.; Flamigni, L. *Angew. Chem., Int. Ed.* **2000**, *39*, 1292−1295.
(17) Collin, J. P.; Harriman, A.; Heitz, V.; Odobel, F.; Sauvage, J. P. *J. Am. Chem. Soc.* **1994**, *116*, 5679−5690.
(18) Andersson, M.; Linke, M.; Chambron, J. C.; Davidsson, J.; Heitz, V.; Hammarström, L.; Sauvage, J. P. *J. Am. Chem. Soc.* **2002**, *124*, 4347−4362.
(19) Andersson, M.; Linke, M.; Chambron, J. C.; Davidsson, J.; Heitz, V.; Sauvage, J. P.; Hammarström, L. *J. Am. Chem. Soc.* **2000**, *122*, 3526−3527.

infrared (TRIR) spectroscopy that porphyrins appended with quinones and diimides can undergo subpicosecond photoinduced charge separation is therefore of particular note.[20−22]

One of the aims of many studies of photoinduced electron transfer in supramolecular assemblies is to produce a long-lived charge-separated state as a mimic of photosynthesis. In this paper, we address the rate of photoinduced charge separation and the lifetime of the charge-separated state in assemblies with a transition metal center linked to a metalloporphyrin. Our studies demonstrate ultrafast charge separation and a short-lived charge-separated state via time-resolved infrared spectroscopy. Conventional expectations would exclude this system for productive reaction, yet we have already shown that one of these assemblies reacts photochemically at a site remote from the chromophore.[23] The implication is that short-lived charge-separated states may react usefully, if they are linked to a sacrificial electron donor.

A transition metal center linked to an organic chromophore such as a porphyrin greatly expands the number of electron or energy transfer reactions that can take place within the assembly compared to pure organic or pure inorganic/organometallic systems. To date, few mixed porphyrin transition metal donor-bridge-acceptor complexes have undergone detailed photophysical examination. Nevertheless, photoinduced redox processes have been reported for several porphyrins linked to transition metal centers.[16,24−33]

Porphyrins with appended metal carbonyl units form a less studied class of compounds. Photophysical data are available for several of these including the notable studies by Hupp et al. and by Alessio and Scandola.[25,34−41] Others have not been investigated photophysically.[42−47]

Rhenium tricarbonyl polypyridine complexes are exceedingly useful both as luminophores[48−58] and as electron acceptors. Their redox properties have been studied very extensively, especially because of the discovery that they mediate the reduction of CO_2.[59−62] The effect of reduction on their structure-sensitive IR bands has been documented by spectroelectrochemical methods and it has been shown that ions of the type *fac*-[Re(CO)$_3$(py)(bpy)]$^+$ are reduced at the bipyridine site.[63−66] Potential electron donors may be linked to the *fac*-[Re(CO)$_3$(py)(bpy)]$^+$ complex via either the bipyridyl unit or the pyridine substituent.

Time-resolved IR spectroscopy has provided an exceptionally valuable tool for studying excited-state properties, and the technology for picosecond IR spectroscopy has improved dramatically.[67−70] The first metal carbonyl excited states to be studied were rhenium tricarbonyl polypyridine derivatives, and there is now an extensive body of data, documenting the effect of various types of transition.[68,71−74]

(20) Kang, Y. K.; Rubtsov, I. V.; Iovine, P. M.; Chen, J.; Therien, M. J. *J. Am. Chem. Soc.* **2002**, *124*, 8275−8279.
(21) Redmore, N. P.; Rubtsov, I. V.; Therien, M. J. *Inorg. Chem.* **2002**, *41*, 566−570.
(22) Rubtsov, I., V.; Kang, Y., K.; Redmore, N., P.; Allen, R., M.; Zheng, J.; Beratan, D. N.; Therien, M., J. *J. Am. Chem. Soc.* **2004**, *126*, 5022−5023.
(23) Gabrielsson, A.; Hartl, F.; Lindsay Smith, J. R.; Perutz, R. N. *Chem. Commun.* **2002**, 950−951.
(24) Flamigni, L.; Marconi, G.; Dixon, I. M.; Collin, J. P.; Sauvage, J. P. *J. Phys. Chem. B* **2002**, *106*, 6663−6671.
(25) Dixon, I. M.; Collin, J. P.; Sauvage, J. P.; Flamigni, L. *Inorg. Chem.* **2001**, *40*, 5507−5517.
(26) Flamigni, L.; Dixon, I. M.; Collin, J. P.; Sauvage, J. P. *Chem. Commun.* **2000**, 2479−2480.
(27) Flamigni, L.; Barigelletti, F.; Armaroli, N.; Ventura, B.; Collin, J. P.; Sauvage, J. P.; Williams, J. A. G. *Inorg. Chem.* **1999**, *38*, 661−667.
(28) Flamigni, L.; Barigelletti, F.; Armaroli, N.; Collin, J. P.; Sauvage, J. P.; Williams, J. A. G. *Chem.−Eur. J.* **1998**, *4*, 1744−1754.
(29) Flamigni, L.; Armaroli, N.; Barigelletti, F.; Balzani, V.; Collin, J. P.; Dalbavie, J. O.; Heitz, V.; Sauvage, J. P. *J. Phys. Chem. B* **1997**, *101*, 5936−5943.
(30) Harriman, A.; Odobel, F.; Sauvage, J. P. *J. Am. Chem. Soc.* **1995**, *117*, 9461−9472.
(31) Harriman, A.; Hissler, M.; Trompette, O.; Ziessel, R. *J. Am. Chem. Soc.* **1999**, *121*, 2516−2525.
(32) LeGourrierec, D.; Andersson, M.; Davidsson, J.; Mukhtar, E.; Sun, L. C.; Hammarström, L. *J. Phys. Chem. A* **1999**, *103*, 557−559.
(33) Monnereau, C.; Gomez, J.; Blart, E.; Odobel, F.; Wallin, S.; Fallberg, A.; Hammarström, L. *Inorg. Chem.* **2005**, *44*, 4806−4817.
(34) Slone, R. V.; Hupp, J. T. *Inorg. Chem.* **1997**, *36*, 5422−5423.
(35) Slone, R. V.; Benkstein, K. D.; Belanger, S.; Hupp, J. T.; Guzei, I. A.; Rheingold, A. L. *Coord. Chem. Rev.* **1998**, *171*, 221−243.
(36) Prodi, A.; Kleverlaan, C. J.; Indelli, M. T.; Scandola, F.; Alessio, E.; Iengo, E. *Inorg. Chem.* **2001**, *40*, 3498−3504.
(37) Prodi, A.; Indelli, M. T.; Kleverlaan, C. J.; Scandola, F.; Alessio, E.; Gianferrara, T.; Marzilli, L. G. *Chem.−Eur. J.* **1999**, *5*, 2668−2679.
(38) Prodi, A.; Indelli, M. T.; Kleverlaan, C. J.; Alessio, E.; Scandola, F. *Coord. Chem. Rev.* **2002**, *229*, 51−78.
(39) Benniston, A. C.; Chapman, G. M.; Harriman, A.; Mehrabi, M. *J. Phys. Chem. A* **2004**, *108*, 9026−9036.
(40) Duncan, T. V.; Rubtsov, I. V.; Uyeda, H. T.; Therien, M. J. *J. Am. Chem. Soc.* **2004**, *126*, 9474−9475.
(41) Prodi, A.; Chiorboli, C.; Scandola, F.; Iengo, E.; Alessio, E.; Dobrawa, R.; Würthner, F. *J. Am. Chem. Soc.* **2005**, *127*, 1454−1462.
(42) Märkl, G.; Reiss, M.; Kreitmeier, P.; Nöth, H. *Angew. Chem., Int. Ed. Engl.* **1995**, *34*, 2230−2234.
(43) Gogan, N. J.; Siddiqui, Z. U. *Can. J. Chem.* **1972**, *50*, 720−725.
(44) Gogan, N. J.; Siddiqui, Z. U. *Chem. Commun.* **1970**, 284−285.
(45) Darling, S. L.; Goh, P. K. Y.; Bampos, N.; Feeder, N.; Montalti, M.; Prodi, L.; Johnson, B. F. G.; Sanders, J. K. M. *Chem. Commun.* **1998**, 2031−2032.
(46) Kariya, N.; Imamura, T.; Sasaki, Y. *Inorg. Chem.* **1998**, *37*, 1658−1660.
(47) Funatsu, K.; Imamura, T.; Ichimura, A.; Sasaki, Y. *Inorg. Chem.* **1998**, *37*, 4986−4995.
(48) Wrighton, M. S.; Morse *J. Am. Chem. Soc.* **1974**, *96*, 988.
(49) Kalyanasundaram, K. *J. Chem. Soc., Faraday Trans. 2* **1986**, *82*, 2401−2415.
(50) MacQueen, D. B.; Schanze, K. S. *J. Am. Chem. Soc.* **1991**, *113*, 6108−6110.
(51) Shen, Y. B.; Sullivan, B. P. *Inorg. Chem.* **1995**, *34*, 6235−6236.
(52) Yam, V. W. W.; Wong, K. M. C.; Lee, V. W. M.; Lo, K. K. W.; Cheung, K. K. *Organometallics* **1995**, *14*, 4034−4036.
(53) Costa, I.; Fabbrizzi, L.; Pallavicini, P.; Poggi, A.; Zani, A. *Inorg. Chim. Acta* **1998**, *276*, 117−121.
(54) Uppadine, L. H.; Redman, J. E.; Dent, S. W.; Drew, M. G. B.; Beer, P. D. *Inorg. Chem.* **2001**, *40*, 2860−2869.
(55) Lewis, J. D.; Moore, J. N. *J. Chem. Soc., Dalton Trans.* **2004**, 1376−1385.
(56) Lewis, J. D.; Bussotti, L.; Foggi, P.; Perutz, R. N.; Moore, J. N. *J. Phys. Chem. A* **2002**, *106*, 12202−12208.
(57) Lewis, J. D.; Perutz, R. N.; Moore, J. N. *J. Phys. Chem. A* **2004**, *108*, 9037−9047.
(58) Peacock, A. F. A.; Batey, H. D.; Raendler, C.; Whitwood, A. C.; Perutz, R. N.; Duhme-Klair, A. K. *Angew. Chem., Int. Ed.* **2005**, *44*, 1712−1714.
(59) Hawecker, J.; Lehn, J.-M.; Ziessel, R. *J. Chem. Soc., Chem. Commun.* **1983**, 536−538.
(60) Kutal, C.; Weber, M. A.; Ferraudi, G.; Geiger, D. *Organometallics* **1985**, *4*, 2161−2166.
(61) Scheiring, T.; Klein, A.; Kaim, W. *J. Chem. Soc., Perkin Trans. 2* **1997**, 2569−2571.
(62) Koike, K.; Hori, H.; Ishizuka, M.; Westwell, J. R.; Takeuchi, K.; Ibusuki, T.; Enjouji, K.; Konno, H.; Sakamoto, K.; Ishitani, O. *Organometallics* **1997**, *16*, 5724−5729.
(63) Stor, G. J.; Hartl, F.; van Outersterp, J. W. M.; Stufkens, D. J. *Organometallics* **1995**, *14*, 1115−1131.
(64) van Outersterp, J. W. M.; Hartl, F.; Stufkens, D. J. *Organometallics* **1995**, *14*, 3303−3310.
(65) Johnson, F. P. A.; George, M. W.; Hartl, F.; Turner, J. J. *Organometallics* **1996**, *15*, 3374−3387.
(66) Paolucci, F.; Marcaccio, M.; Paradisi, C.; Roffia, S.; Bignozzi, C. A.; Amatore, C. *J. Phys. Chem. B* **1998**, *102*, 4759−4769.
(67) Kuimova, M. K.; Alsindi, W. Z.; Dyer, J.; Grills, D. C.; Jina, O. S.; Matousek, P.; Parker, A. W.; Portius, P.; Sun, X. Z.; Towrie, M.; Wilson, C.; Yang, J. X.; George, M. W. *Dalton Transactions* **2003**, 3996−4006.
(68) Vlček, A., Jr.; Farrell, I. R.; Liard, D. J.; Matousek, P.; Towrie, M.; Parker, A. W.; Grills, D. C.; George, M. W. *J. Chem. Soc., Dalton Trans.* **2002**, 701−712.
(69) Matousek, P.; Towrie, M.; Stanley, A.; Parker, A. W. *Appl. Spectrosc.* **1999**, *53*, 1485−1489.
(70) Towrie, M.; Grills, D. C.; Dyer, J.; Weinstein, J. A.; Matousek, P.; Barton, R.; Bailey, P. D.; Subramaniam, N.; Kwok, W. M.; Ma, C. S.; Phillips, D.; Parker, A. W.; George, M. W. *Appl. Spectrosc.* **2003**, *57*, 367−380.
(71) Glyn, P.; George, M. W.; Hodges, P. M.; Turner, J. J. *J. Chem. Soc., Chem. Commun.* **1989**, 1655−1657.
(72) Schoonover, J. R.; Strouse, G. F. *Chem. Rev.* **1998**, *98*, 1335−1355.

Chart 1

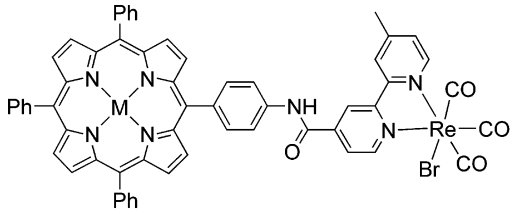

$Re(CO)_3BrBpy$-MTPP

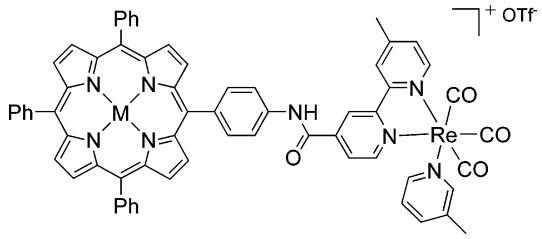

$[Re(CO)_3(Pic)Bpy$-MTPP$][OTf]$ M = Mg, Zn

We have previously described zinc porphyrin systems linked via an amide spacer to tungsten pentacarbonyl pyridine and rhenium tricarbonyl 2,2′-bipyridine bromide.[75,76] This design allows the porphyrin moiety to be monitored by absorption and emission spectroscopy, while the transition metal unit is revealed by its structure-sensitive CO-stretching modes. The rhenium tricarbonyl bromide complex **$[Re(CO)_3BrBpy$-ZnTPP$]$** (Chart 1), however, has two disadvantages: first, it does not undergo photoinduced reaction with intermolecular electron donors such as triethylamine,[23] and second, its solubility is very low in common solvents. In the second generation complexes, we aimed to increase solubility and increase the free energy of electron transfer from metalloporphyrin to rhenium bipyridine by replacing the bromine substituent with the 2-electron donor, 3-picoline.[23] We showed that irradiation of the resulting **$[Re(CO)_3(Pic)Bpy$-ZnTPP$][OTf]$** (Chart 1) into the long-wavelength porphyrin absorption bands caused reaction at the remote rhenium picoline site in the presence of triethylamine. We showed that this excitation of the porphyrin resulted in electron transfer from the porphyrin to the rhenium 2,2′-bipyridine center that initiated reaction. This assembly may be considered as a dyad without triethylamine or a triad with it. It exhibits photoinduced reaction at a site remote from the chromophore, one of the categories of photoactive supramolecule recognized by Balzani and Scandola.[1]

In this paper, we report the photophysics of **$[Re(CO)_3(Pic)$-Bpy-ZnTPP$][OTf]$** and **$[Re(CO)_3(Pic)Bpy$-MgTPP$][OTf]$** (Chart 1) and provide the first detailed time-resolved transient absorption and infrared study of a porphyrin appended with a transition metal carbonyl moiety. We demonstrate that photoinduced charge separation from the excited porphyrin to Re(bpy) can occur on a picosecond time scale and that the fast charge-recombination results in a vibrationally excited ground state. We show how this short lifetime can be reconciled with reactivity at the remote site.

Experimental Section

General Procedures. Chemicals were obtained from the following suppliers: benzophenone (Acros Organics); $Re_2(CO)_{10}$, Celite, activated alumina, diisopropylethylamine, ferrocene, 3-picoline, $[Bu_4N][PF_6]$, and anhydrous magnesium bromide (Aldrich); zinc acetate, magnesium sulfate, sodium carbonate, and thionyl chloride (Fisons); silver trifluoromethanesulfonate (Avocado); silica gel 60 and TLC plates F_{254} (Merck).

Solvents for general use were used as obtained from Fisher. Solvents for Schlenk-line work were dried by refluxing over sodium/benzophenone (benzene, toluene, pentane, THF), over P_2O_5 (acetonitrile, butyronitrile), or over $CaCl_2$ and then P_2O_5 (dichloromethane). After refluxing they were distilled and stored under argon. Triethylamine (BDH) was dried over CaH_2 and stored over 4 Å molecular sieves.

$CDCl_3$ and CD_2Cl_2 were either used as obtained from Fluorochem or Goss or dried over P_2O_5. Pyridine-d_5 (Aldrich) was dried over 4 Å molecular sieves. Dried NMR solvents were transferred into an NMR tube fitted with a ptfe stopcock (Young) on a high-vacuum line and sealed under argon.

Syntheses. 5-[4-(4-Methyl-2,2′-bipyridine-4′-carboxyamidyl)phenyl]-10,15,20-triphenylporphyrin: Bpy-H_2TPP. Abbreviations are shown in Chart 1 and Scheme 1. 4-Methyl-2,2′-bipyridine-4′-carboxylic acid (0.21 g, 0.98 mmol), synthesized according to a literature procedure,[77a] was heated at reflux in thionyl chloride (6 cm^3) under an inert atmosphere overnight. Excess thionyl chloride was removed in vacuo; the resulting yellow solid was dried for a further 30 min, and triethylamine (20 cm^3, dry) was added. **NH_2-H_2TPP** was synthesized by nitration of tetraphenylporphyrin,[77b] followed by reduction.[77c] A solution of **NH_2-H_2TPP** (0.77 g, 1.22 mmol) in dichloromethane (50 cm^3, dry) was added by cannula, and the reaction mixture was stirred for 1 h at room temperature and then heated for 2.5 h at reflux. The solvent was removed, and the purple solid was purified by column chromatography (Si-60, dichloromethane, dichloromethane with 4% methanol). The second fraction was collected, the solvent was removed, and the purple solid was recrystallized by slow evaporation of an ethanol dichloromethane mixture (1:1 v/v) to yield the desired compound **Bpy-H_2TPP** (0.5 g, 0.61 mmol, 62%). The ^{1}H NMR spectrum was in good agreement with that reported earlier.[78]

^{1}H NMR (500 MHz, THF-d_8): δ −2.78 (2 H, br, s, inner NH); 2.32 (3 H, s, Bpy CH_3); 7.10 (1 H, d, J 4.9 Hz, Bpy); 7.60−7.66 (9 H, m, *p*-, *m*-phenyl); 7.83 (1 H, dd, J 4.9 Hz, J 0.6 Hz Bpy); 8.18 (2 H, d, J 8.1 Hz, *m*-bridging phenyl); 8.07−8.12 (8 H, m, 6 *o*-phenyl and 2 bridging phenyl); 8.32 (1 H, s, Bpy); 8.43 (1 H, d, J 4.77 Hz, 1 Bpy); 8.69−8.73 (7 H, m, 6 β- pyrrolic H and 1 Bpy); 8.80 (2 H, br, β-pyrrolic); 9.00 (1 H, s, Bpy); 10.41 (1 H, s, br, CONH).

UV/vis (THF): λ_{max}/nm (ϵ/dm^3 mol^{-1} cm^{-1}) = 373 (31 000), 416 (31 000), 514 (19 800), 549 (11 100), 592 (6900), 647 (5900).

ESI-MS: m/z = 826 (100% MH^+).

High-resolution FAB-MS: For $[C_{56}H_{39}N_7O]^+$, observed mass 825.3221, calculated mass 825.3216, difference 0.5 mD. In this and other syntheses, high-resolution mass spectrometry was used in preference to elemental analysis because of unreliable results with elemental analysis of metalloporphyrins.

5-{4-[Rhenium(I)tricarbonyl(3-picoline)-4-methyl-2,2′-bipyridine-4′-carboxyamidyl]phenyl}-10,15,20-triphenylporphyrinatozinc(II) Trifluoromethanesulfonate; $[Re(CO)_3(Pic)$Bpy-ZnTPP$][OTf]$. $Re(CO)_3BrBpy$-ZnTPP (0.10 g, 0.081 mmol), synthesized from **Bpy-**

(73) Dattelbaum, D. M.; Omberg, K. M.; Hay, J. P.; Gebhart, N. L.; Martin, R. L.; Schoonover, J. R.; Meyer, T. J. *J. Phys. Chem. A* **2004**, *108*, 3527−3536.
(74) George, M. W.; Turner, J. J. *Coord. Chem. Rev.* **1998**, *177*, 201−217.
(75) Aspley, C. J.; Lindsay Smith, J. R.; Perutz, R. N.; Pursche, D. *J. Chem. Soc., Dalton Trans.* **2002**, 170−180.
(76) Aspley, C. J.; Lindsay Smith, J. R.; Perutz, R. N. *J. Chem. Soc., Dalton Trans.* **1999**, 2269−2271.
(77) (a) McCafferty, D. G.; Bishop, B. M.; Wall, C. G.; Hughes, S. G.; Mecklenberg, S. L.; Meyer, T. J.; Erickson, B. W. *Tetrahedron* **1995**, *51*, 1093−1106. (b) Kruper, W. J.; Chamberlin, T. A.; Kochanny, M. *J. Org. Chem.* **1989**, *54*, 2753−2756. (c) Baldwin, J. E.; Crossley, M. J.; DeBernardis, J. *Tetrahedron*, **1982**, *38*, 685−692.
(78) Aspley, C. J. Ph.D. Thesis, University of York, York, U.K., 2000.

Scheme 1. Synthesis of **[Re(CO)$_3$(pic)Bpy-MTPP][OTf]** (M = Zn, Mg)

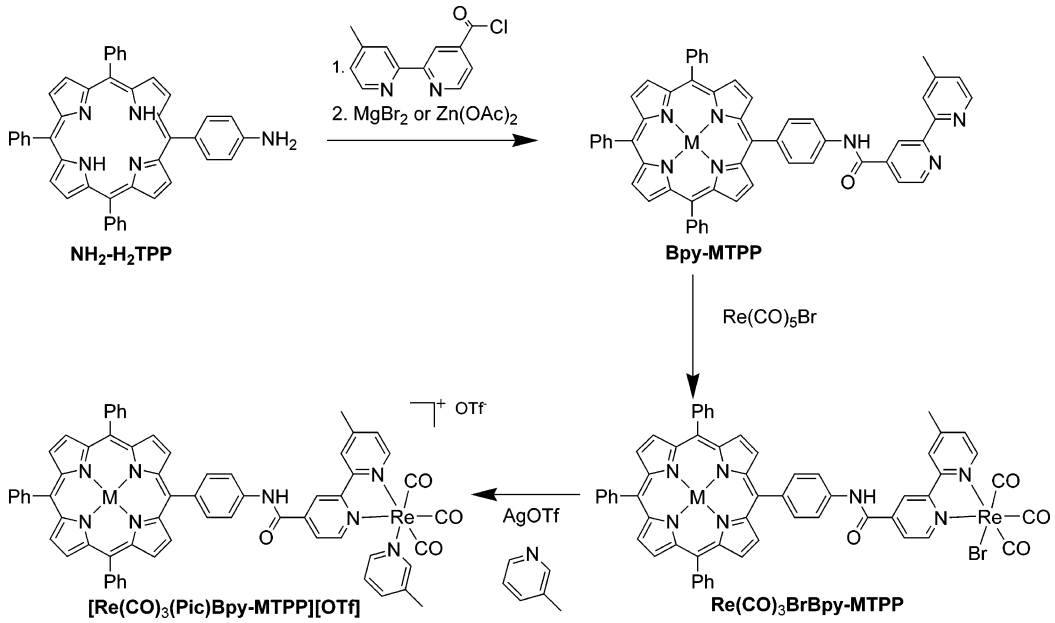

ZnTPP (see Supporting Information) according to the method of Aspley et al.,[76,78] was dissolved in a mixture of tetrahydrofuran (10 cm^3, dry); 3-picoline (0.5 cm^3) and AgOTf (0.1 g, 0.4 mmol) were added. The reaction mixture was heated under argon at reflux for 1 h. The solvent was removed in vacuo, and the solid was redissolved in dichloromethane (3 cm^3) and purified by column chromatography (Si-60, dichloromethane with 20% v/v tetrahydrofuran), to yield **[Re(CO)$_3$(Pic)Bpy-ZnTPP][OTf]** (0.10 g, 0.071 mmol, 88%).

IR (ν/cm^{-1}) (THF) 2031 (s), 1927 (s, broad) (ν(CO)).

^{1}H NMR (400 MHz, CD_2Cl_2): δ 2.30 (3 H, s, Bpy CH_3); 2.75 (3 H, 3-picoline CH_3); 7.27 (1 H, dd, *J* 7.8 and 5.9 Hz, 3-picoline H_2); 7.60 (1 H, d, *J* 5.9 Hz, Bpy H_5'); 7.67 (1 H, d, *J* 7.8 Hz, 3-picoline H_4); 7.80 (9 H, m, 9 *m*-, *p*-phenyl); 7.95 (1 H, d, *J* 5.9 Hz 3-picoline H_6); 8.14 (1 H, s, 3-picoline H_2); 8.27 (10 H, m, 6 *o*-phenyl and 4 bridging C_4H_6); 8.38 (1 H, d, *J* 5.9 Hz, Bpy H_5); 8.72 (1 H, s, Bpy H_3'); 8.92 (4 H, s, β-pyrrolic H_a and H_b); 8.94 (2 H, d, *J* 4.9 Hz, β-pyrrolic H_c); 9.00 (1 H d, *J* 5.9 Hz Bpy H_6' overlaps with doublet at 9.01 ppm); 9.01 (2 H, d, *J* 4.9 Hz, β-pyrrolic H_d); 9.19 (1 H, s, Bpy H_3); 9.33 (1 H, d, *J* 5.9 Hz, Bpy H_6) 10.66 (1 H, s, br, CONH).

ESI-MS: *m*/*z* = 1253 (100% [M, major contribution from $C_{65}H_{44}N_8O_4{}^{187}Re^{66}Zn]^+$), 1160 (10% [M − 3-picoline]$^+$).

High-resolution ESI-MS: For isotopomer, $[C_{65}H_{44}N_8O_4{}^{185}Re^{64}Zn]^+$ observed mass, 1249.2301, calculated mass1249.2298, difference 0.3 mDa

5-[4-(4-Methyl-2,2′-bipyridine-4′-carboxyamidyl)phenyl]-10,15,-20-triphenylporphyrinatomagnesium(II): Bpy-MgTPP. A literature procedure was adapted for the insertion of magnesium into **Bpy-H$_2$TPP**.[79,80] **Bpy-H$_2$TPP** (0.200 g, 0.24 mmol) was dissolved in trichloromethane (30 cm^3); diisopropylethylamine (1 cm^3) and magnesium bromide (anhydrous 0.44 g, 2.4 mmol) were added. The reaction mixture was stirred at room temperature, and a purple precipitate formed after a few minutes; the precipitate dissolved upon addition of diethyl ether (5 cm^3, dry). The reaction was stirred for 20 min at room temperature, diluted with dichloromethane (50 cm^3), washed with sodium carbonate solution (5%, 150 cm^3), and dried ($MgSO_4$), and the solvent was removed in vacuo. The blue-purple product was purified by column chromatography (alumina neutral Brockman grade 1, poured in dichloromethane and eluted with dichloromethane/tetrahydrofuran, 2/1 v/v) to give **Bpy-MgTPP** as a blue-purple solid (0.1 g, 0.12 mmol, 50%). The ^{1}H NMR spectrum of **Bpy-MgTPP** was best resolved in pyridine-d_5 (Table S1, Supporting Information).

^{1}H NMR (500 MHz, pyridine-d_5): δ 2.15 (3 H, s, Bpy CH_3); 7.02 (1 H, d, *J* 4.64 Hz, Bpy), 7.66 (9 H, m, *p*-, *m*-phenyl); 8.14 (1 H, d, *J* 5.00 Hz, Bpy); 8.30 (6 H, m, *o*-phenyl); 8.35 (2 H, d, *J* 8.30 Hz, *m*-bridging phenyl); 8.43 (1 H, s, Bpy); 8.48 (2 H, d, *J* 8.30 Hz, *m*-bridging phenyl); 8.55 (1 H, d, *J* 4.9 Hz, 1 Bpy); 8.87 (1 H, d, *J* 4.64 Hz, Bpy); 9.02 (4 H, s, β-pyrrolic); 9.02 (2 H, d, *J* 4.64 Hz, β-pyrrolic); 9.06 (2 H, d, *J* 4.64 Hz, β-pyrrolic); 9.48 (1 H, s, Bpy); 11.80 (1 H, s, CONH)

ESI-MS: *m*/*z* = 849 (100% MH$^+$).

High-Resolution FAB-MS: For $[C_{56}H_{37}N_7OMg]^+$, observed mass 847.2907, calculated mass 847.2907, difference 0.0 mDa.

5-{4-[Rhenium(I)tricarbonylbromide-4-methyl-2,2′-bipyridine-4′-carboxyamidyl]phenyl}-10,15,20-triphenylporphyrinatomagnesium(II): Re(CO)$_3$BrBpy-MgTPP. Rhenium pentacarbonyl bromide (0.030 g, 0.073 mmol) and **Bpy-MgTPP** (0.050 g, 0.059 mmol) were heated in toluene (30 cm^3, dry) at 70 °C under argon for 5 h. After a black precipitate had formed, the reaction mixture was left overnight before the solvent was removed in vacuo. The residue was washed with methanol (10 cm^3) and diethyl ether (10 cm^3) yielding a dark purple product that was used without further purification in the next step.

5-{4-[Rhenium(I)tricarbonyl(3-picoline)-4-methyl-2,2′-bipyridine-4′-carboxyamidyl]phenyl}-10,15,20-triphenylporphyrinatomagnesium(II) Trifluoromethanesulfonate: [Re(CO)$_3$(Pic)Bpy-MgTPP][OTf]. Re(CO)$_3$BrBpy-MgTPP (0.070 g, 0.059 mmol) was suspended in dry tetrahydrofuran (10 cm^3); 3-picoline (0.2 cm^3) and silver trifluoromethanesulfonate (0.075 g, 0.295 mmol) were added. The reaction mixture was heated under argon at reflux for 1 h before the solvent was removed, and the solid was redissolved in tetrahydrofuran (10 cm^3). The solution was filtered through a plug of alumina (eluted with tetrahydrofuran with 0.5% v/v triethylamine), and the solvent was removed to give **[Re(CO)$_3$(Pic)Bpy-MgTPP][OTf]** (0.068 g, 0.05 mmol, 85%).

IR (ν/cm^{-1}) (THF) 2031(s), 1927 (s, broad). (PrCN): 2033 (s), 1927 (s, broad) (ν(CO)).

^{1}H NMR (500 MHz, CD_2Cl_2): δ 2.30 (3 H, s, Bpy CH_3); 2.75 (3 H, 3-picoline CH_3); 7.26 (1 H, dd, *J* 7.8 and 5.9 Hz, 3-picoline H_2); 7.61 (1 H, d, *J* 5.9 Hz, Bpy H_5'); 7.67 (1 H, d, *J* 7.8 Hz, 3-picoline H_4); 7.80 (9 H, m, 9 *m*-, *p*-phenyl); 7.95 (1 H, d, *J* 5.9 Hz, 3-picoline H_6); 8.14 (1 H, s, 3-picoline H_2); 8.27 (10 H, m, 6 *o*-phenyl and 4 bridging C_4H_6); 8.38 (1 H, d, *J* 5.9 Hz, Bpy H_5); 8.72 (1 H, s, Bpy H_3'); 8.94 (4

(79) Lindsey, J. S.; Woodford, J. N. *Inorg. Chem.* **1995**, *34*, 1063−1069.
(80) Oshea, D. F.; Miller, M. A.; Matsueda, H.; Lindsey, J. S. *Inorg. Chem.* **1996**, *35*, 7325−7338.

H, s, β-pyrrolic H_a and H_b); 8.96 (2 H, d, *J* 4.9 Hz, β-pyrrolic H_c); 9.00 (1 H, d, *J* 5.9 Hz Bpy H_6' overlaps with doublet at 9.03 ppm): 9.03 (2 H, d, *J* 4.9 Hz, β-pyrrolic H_d); 9.19 (1 H, s, Bpy H_3); 9.33 (1 H, d, *J* 5.9 Hz, Bpy H_6) 10.66 (1 H, s, br, CONH).

ESI-MS: $m/z = 1211$ (100% M^+), (30% $[M - (3\text{-Pic})]^+$).

High-Resolution FAB-MS: For $[C_{65}H_{44}N_8O_4Mg^{185}Re]^+$ isotopomer, observed mass 1209.2865, calculated mass 1209.2866, difference 0.1 mDa.

Steady-State Spectroscopy. Infrared spectra were recorded on a Mattson RS FTIR instrument with the solvent spectrum as background. FAB mass spectra (both low and high resolution) were recorded on a VG AutoSpec mass spectrometer and an ESI mass spectra on a Finnigan LCQ instrument. High-resolution ESI spectra were recorded by the EPSRC National Mass Spectrometry Service Centre in Swansea, UK. NMR spectra were recorded on a JEOL EX 270, Bruker MSL 300, or Bruker AMX 500 spectrometer. UV−visible spectra were recorded on a Perkin-Elmer Lambda 7 or Hewlett-Packard 8452A spectrophotometer. Emission spectra were recorded with a Jobin Yvon-Spex Fluoromax-2 spectrometer with right angle illumination (typically slit widths for both emission and excitation 2 nm). Spectra were corrected for photomultiplier response by using the correction file supplied by the manufacturer. When spectra were recorded under inert atmosphere, samples were placed in a cuvette equipped with a bulb attached via sidearm and a ptfe stopcock and were degassed by three consecutive freeze−pump−thaw cycles and backfilled with argon.

Electrochemistry. Cyclic voltammograms were recorded with a PAR EG&G model 283 potentiostat, using an airtight single-compartment cell placed in a Faraday cage. The working electrode was a Pt microdisk (0.42 mm^2 apparent surface area), polished with a 0.25 μm diamond paste between the scans. Coiled Pt and Ag wires served as an auxiliary and pseudoreference electrode, respectively. The concentration of the analyte was 10^{-3} mol dm^{-3}. Ferrocene (Fc) was used as the internal standard.[81] The supporting electrolyte, $[Bu_4N][PF_6]$, was recrystalized twice from absolute EtOH and dried overnight under vacuum at 80 °C before use.

IR and UV/vis spectroelectrochemistry at room temperature was conducted with an Optically Transparent Thin-Layer Electrochemical (OTTLE) cell.[82] The concentrations of the solutions were 10^{-1} mol dm^{-3} in the supporting electrolyte and 5×10^{-3} mol dm^{-3} (IR) or 10^{-3} mol dm^{-3} (UV/vis) in the analyte. The working electrode potential of the spectroelectrochemical cells was controlled with a PA4 potentiostat (EKOM, Polná, Czech Republic). The IR spectra were recorded with a Bio-Rad FTS-7 spectrometer (16 scans, 2 cm^{-1} spectral resolution), and the UV/vis spectra, with a HP 8453A diode array spectrophotometer.

Ultrafast Visible Absorption Experiments. The time-resolved visible (TRVIS) absorption experiments were performed with the University of Amsterdam ultrafast spectroscopy setup with a pump wavelength of 560 nm.[83] The energies of the pump and probe pulses were <5 μJ per pulse and 5 nJ per pulse, respectively, and the angle between the pump and probe pulses was between 7° and 10°. To avoid local heating, the circular cell (Hellma $d = 18$ mm, $l = 1$ mm) was placed in a homemade rotating mount (1000 rpm). Between 200 and 500 pulses were averaged to provide one spectrum at a particular time. The wavelength interval between points was 1.4 nm. Data were collected for 300 delay times. The total instrument rise-time was approximately 200 fs.[83] The samples were prepared with an optical density of ca. 0.9 at the excitation wavelength. Experiments were performed under the magic angle condition in order to circumvent effects from the reorientation of the solute. The ground-state electronic absorption spectra were recorded before and after the ultrafast experiment, and in no case was any photodecomposition observed. The transient decay was fitted to a single-exponential function.

Nanosecond Absorption Experiments. The York nanosecond absorption equipment has been described previously.[84] The solutions were excited with the second harmonic of a Quanta-Ray 3 Nd:YAG laser (pulse length 10 ns) and detected with a pulsed arc lamp, monochromator, and photomultiplier linked to a digital oscilloscope.

Ultrafast Infrared Experiments. Time-resolved infrared (TRIR) measurements were performed on the PIRATE equipment that has been described in detail previously.[68−70,85,86] In brief, the sample solution was excited at 560 or 600 nm with an OPA pumped by frequency-doubled pulses from a Ti:sapphire laser of ~150 fs duration (fwhm) and ca. 1 μJ energy focused to a spot of ca. 150 μm. The samples were probed with IR (~150 fs) pulses obtained by difference-frequency generation. The IR probe pulses cover spectral ranges ca. 200 cm^{-1} wide. The sample solutions in MeCN were flowed through a CaF_2 IR cell, which was rastered in two dimensions. Path lengths of 0.5 to 1 mm were used. All spectral and kinetic fitting procedures were performed using Microcal Origin 7 software. A germanium filter was placed in front of the detector to remove scattered excitation light.

Results

Synthetic Methodology. The synthetic strategy for **[Re(CO)$_3$(Pic)Bpy-MTPP][OTf]** (M = Zn, Mg) is depicted in Scheme 1. The synthesis of **Re(CO)$_3$BrBpy-ZnTPP** has been described previously,[76,78] but an altered and higher yielding procedure is presented for its precursors **Bpy-H$_2$TPP** (see Experimental) and **Bpy-ZnTPP** (see Supporting Information). The rhenium-appended complex **Re(CO)$_3$BrBpy-ZnTPP** was converted to the 3-picoline derivative **[Re(CO)$_3$(Pic)Bpy-ZnTPP][OTf]** by a standard method of reaction with 3-picoline and silver triflate in THF at reflux.

Magnesium ions were inserted into **Bpy-H$_2$TPP** by the heterogeneous method developed by Lindsey et al. yielding **Bpy-MgTPP** under mild conditions.[79,80] **Bpy-MgTPP** is extremely acid-sensitive, and chromatography over silica regenerated the free-base compound **Bpy-H$_2$TPP** quantitatively. The rhenium chelate **Re(CO)$_3$BrBpy-MgTPP** was made by heating the ligand and $Re(CO)_5Br$ in benzene or toluene.[48,76,78] Since **Re(CO)$_3$BrBpy-MgTPP** was only soluble in coordinating solvents such as DMF and pyridine, it was converted directly to the 3-picoline derivative **[Re(CO)$_3$(pic)Bpy-MgTPP][OTf]** without purification by the same method as that for the zinc porphyrin.

Ground-State Spectroscopy. NMR Spectroscopy. ^{1}H NMR spectra of **[Re(CO)$_3$(Pic)Bpy-ZnTPP][OTf]** were assigned with the aid of NOE and COSY experiments (Supporting Information). The labeling and assignment for the spectrum in CD_2Cl_2 are shown in Figure 1. Not surprisingly, the magnesium derivative displays a very similar spectrum to that of the zinc complex. The two methyl groups resonate at δ 2.30 and 2.75, and the amide N−H proton appears at δ 10.70. The β-pyrrolic protons are shifted by 0.2 ppm downfield relative to the zinc derivative. There were no resonances at negative shift where the free-base inner N−H protons of any residual free-base porphyrin appear, nor were there any resonances due to picoline complexed to magnesium.

UV/vis Absorption Spectra. The UV/vis absorption spectrum of **Bpy-ZnTPP** is very similar to that of **ZnTPP**, with one very strong absorption peak observed at 424 nm (Soret band) and two strong transitions at 556 and 596 nm (Q-bands, Table 1).

(81) Gritzner, G.; Kůta, J. *Pure Appl. Chem* **1984**, *56*, 461−466.
(82) Krejčik, M.; Daněk, M.; Hartl, F. *J. Electroanal. Chem. Interfacial Electrochem.* **1991**, *317*, 179−187.
(83) Vergeer, F. W.; Kleverlaan, C. J.; Stufkens, D. J. *Inorg. Chim. Acta* **2002**, *327*, 126−113.
(84) Nicasio, M. C.; Perutz, R. N.; Tekkaya, A. *Organometallics* **1998**, *17*, 5557−5564.

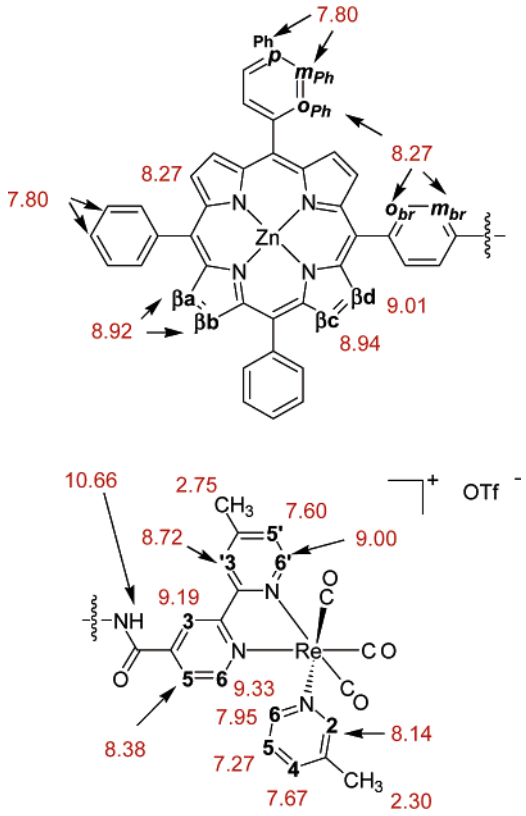

Figure 1. Labeling and chemical shifts for the ^{1}H NMR spectra of **[Re(CO)$_3$(Pic)Bpy-ZnTPP][OTf]** in CD_2Cl_2 shown in two parts.

Table 1. Absorption Maxima (nm) and Molar Absorption Coefficients (dm^3 mol^{-1} cm^{-1}) of Metalloporphyrin Derivatives

compound	Q_1	Q_2	Q_3	Soret
Bpy-ZnTPP	596	556	517	424
	(14 100)	(22 900)	(4340)	(470 000)
[Re(CO)$_3$(Pic)Bpy-ZnTPP]$^+$	596	556	517	424
	(9100)	(21 300)	(3800)	(474 000)
Bpy-MgTPP	614	570	531	430
	(16 400)	(19 300)	(5200)	(490 000)
[Re(CO)$_3$(Pic)Bpy-MgTPP]$^+$	614	570	531	430
	(12 200)	(13 800)	(4500)	(356 000)

The rhenium-appended complex shows only small changes in these porphyrin-based bands. The rhenium-bpy MLCT band and IL absorption are expected around 370 and 300 nm, respectively.[50,56] Although the transitions are masked by the porphyrin transitions, the molar absorption coefficient of **[Re(CO)$_3$(Pic)-Bpy-ZnTPP][OTf]** is higher in this region than that of **Bpy-ZnTPP**. The absorption spectra in different solvents were investigated in an attempt to resolve the rhenium complex transitions from those of the zinc porphyrin. No clear feature assignable to either the IL or MLCT bands of the Re(CO)$_3$-(pic)(bpy) unit emerged upon substituting the solvent or by coordination of *N*-methylimidazole to the zinc porphyrin. The magnesium porphyrin analogues show a long wavelength shift of all bands (Table 1, see Figure S4 in Supporting Information).

IR Spectra. The ground-state infrared spectra of **[Re(CO)$_3$-(Pic)Bpy-ZnTPP][OTf]** and **[Re(CO)$_3$(Pic)Bpy-MgTPP][OTf]** display two bands at 2031 and 1927 cm^{-1} in THF. The a″ and a′(2) bands merge into one broad absorption at 1927 cm^{-1} reflecting the pseudo-C_{3v} geometry around the transition metal. Variation of the solvent from THF to butyronitrile or dichloromethane has little effect on the carbonyl stretching frequencies (less than 2 cm^{-1}).

Cyclic Voltammetry and Spectroelectrochemistry. Data for cyclic voltammetry are listed in Table 2. The oxidation of **[Re(CO)$_3$(Pic)Bpy-ZnTPP][OTf]** and **Bpy-ZnTPP** occurs at the same electrode potential, consistent with porphyrin-based one-electron oxidation. The potential for oxidation of **Bpy-MgTPP** is 140 mV lower. Both **Bpy-MgTPP** and **Bpy-ZnTPP** show chemically reversible reduction (v = 100 mV s^{-1}), whereas the reduction of **[Re(CO)$_3$(Pic)Bpy-ZnTPP][OTf]** in THF is partly chemically irreversible and occurs at a potential 510 mV less negative than that for **Bpy-ZnTPP**. This behavior is consistent with reduction localized at the rhenium bipyridine moiety and some replacement of picoline by the donor solvent.[23] In butyronitrile (PrCN), on the other hand, the reduction of **[Re(CO)$_3$(Pic)Bpy-ZnTPP][OTf]** is fully reversible. The radical product is further reduced to the corresponding anion in a chemically irreversible step at $E_{p,c}$ = −1.77 V vs Fc/Fc$^+$ (not in Table 2), which partly overlaps with the reversible reduction of the remote ZnTPP moiety at −1.83 V.

UV/vis spectroelectrochemistry of **Bpy-ZnTPP** in THF was employed to examine the effect of oxidation on the UV/vis spectrum (See Figure S5 in Supporting Information). The spectrum revealed loss of the Q-band at 596 and 556 nm and gain of absorption in the 450 nm region and a very broad band centered at 630 nm. We can exploit the changes in absorbance to deduce that $\Delta\epsilon_{650}/\Delta\epsilon_{470} \approx 0.6$ and $\Delta\epsilon_{470}$ lies in the range $\Delta\epsilon = 1.8 \times 10^4$ to 3.4×10^4 dm^3 mol^{-1} s^{-1} by employing the value of ϵ at 559 nm for **Bpy-ZnTPP** ($\Delta\epsilon_{450}$ refers to the change in molar absorption coefficient on oxidation at 450 nm, etc.; the two values correspond to extreme values for the absorption coefficient of the radical cation at 559 nm.)

IR spectroelectrochemistry of **[Re(CO)$_3$(Pic)Bpy-ZnTPP]$^+$** was carried out in PrCN at ambient temperature. On reduction, the ν(CO) bands of the precursor at 2035 and 1933 cm^{-1} lost intensity and new bands appeared at 2012 and 1902 cm^{-1}; the latter is very broad like the corresponding band of the precursor (Figure 2). These two bands are assigned to the radical species **[Re$^+$(CO)$_3$(Pic)Bpy$^{\bullet-}$-ZnTPP]** and illustrate the characteristic shift to low frequency (−23 cm^{-1} for the upper band and ca. −31 cm^{-1} for the lower unresolved bands). The thin-layer cyclic voltammogram recorded in the course of the experiment did not reveal any significant substitution of picoline with PrCN, which would otherwise shift the electrode potential more negatively by ca. 100 mV (see Table 2). The changes in absorbance (Figure 2) allow us to estimate that the molar absorption coefficient of the high frequency band of the singly reduced species (2012 cm^{-1}) is approximately 57% that of the corresponding band of the precursor (2035 cm^{-1}). Subsequent irreversible reduction of **[Re$^+$(CO)$_3$(Pic)Bpy$^{\bullet-}$-ZnTPP]** resulted in a mixture of two anionic species **[Re(CO)$_3$(PrCN)Bpy-ZnTPP]$^-$** (major) and **[Re(CO)$_3$Bpy-ZnTPP]$^-$** (minor) characterized by high-frequency bands at 1983 and 1948 cm^{-1}, respectively, and overlapping broad low-frequency bands between 1900 and 1840 cm^{-1}.[63−65]

In agreement with cyclic voltammetry, the reduction of **[Re(CO)$_3$(Pic)Bpy-ZnTPP]$^+$** in THF at room temperature is also irreversible when monitored in situ by IR spectroscopy. The parent complex (ν(CO) at 2033 and 1928 cm^{-1}) converts to the corresponding radical (ν(CO) at 2011, 1906, and 1892 cm^{-1})

Table 2. Cyclic Voltammetry Data, $E_{1/2}$/V vs Fc^+/Fc[a]

compound	$E_{1/2}$(ox)	$E_{1/2}$(red) (bpy-centered)	$E_{1/2}$(red) (porphyrin-centered)
Zn(TPP)	0.43		−1.84
Bpy-ZnTPP	0.38		−1.95
Bpy-MgTPP	0.24		−1.76
[Re(CO)$_3$(Pic)Bpy-ZnTPP][OTf]	0.38	−1.44[b]	
[Re(CO)$_3$(Pic)Bpy-ZnTPP][OTf]/PrCN	0.36	−1.41	−1.83
[Re(CO)$_3$(Pic)(bpy)][OTf]		−1.47[c]	
[Re(CO)$_3$(PrCN)(bpy)][OTf]		−1.58	
[Re(CO)$_3$(THF)(bpy)][OTf][b]		−1.69[d]	

[a] Conditions: in THF unless otherwise stated containing $[Bu_4N][PF_6]$ (10^{-1} mol dm^{-3}), working electrode Pt disk, $T = 298$ K. [b] Partly chemically irreversible. [c] Reference 23. [d] Reference 63.

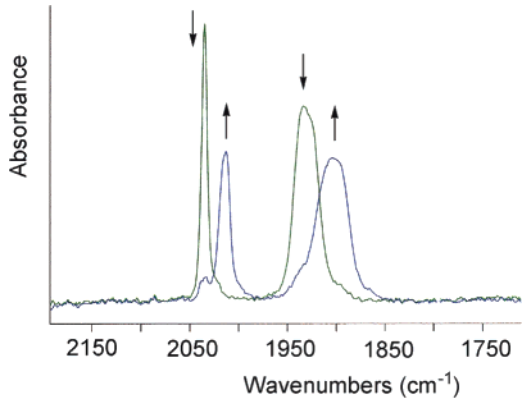

Figure 2. IR spectroelectrochemistry of **[Re(CO)$_3$(Pic)Bpy-ZnTPP][OTf]** in PrCN at room temperature, recorded with an OTTLE cell. Green spectrum: **[Re(CO)$_3$(Pic)Bpy-ZnTPP]$^+$**; blue spectrum **[Re$^+$(CO)$_3$(Pic)-Bpy$^{\bullet-}$-ZnTPP]**. This one-electron-reduced radical is stable under these conditions.

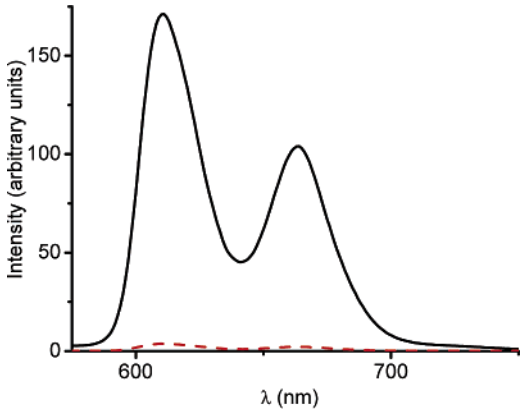

Figure 3. Emission spectra (uncorrected) of **Bpy-MgTPP** (black line) and **[Re(CO)$_3$(Pic)Bpy-MgTPP][OTf]** (red broken line) in MeCN, 560 nm excitation.

which gradually undergoes picoline substitution with solvent molecules, producing the cation **[Re(CO)$_3$(THF)Bpy-ZnTPP]$^+$** (ν(CO) at 2019, 1914, and 1897 cm^{-1}). The latter is reduced at a more negative potential than the parent cationic complex (Table 2).

Steady-State Emission Spectroscopy. Zinc and magnesium porphyrins emit strongly from the first singlet-excited state; simple rhenium tricarbonyl bipyridine complexes are also emissive but exhibit distinctly different spectra.[7,48] As a result, steady state emission spectroscopy is a valuable tool for probing potential perturbations of the excited state of one part of the supramolecule in the presence of the other. Solvent studies can help elucidate the mechanism of emission quenching. If photoinduced electron transfer occurs, a large dipole change ensues and the solvent polarity is expected to have a major impact on the quenching. In contrast, energy transfer is usually less dependent on the solvent polarity. Quenching may also occur through the heavy atom effect, but this does not involve a change in dipole moment and consequently is unaffected by the solvent polarity.

The porphyrin fluorescence of **Bpy-ZnTPP** was found to be identical in band position and intensity to that of **ZnTPP**.[7,48] The emission spectrum of **[Re(CO)$_3$(Pic)Bpy-ZnTPP][OTf]** exhibits two sharp bands at 602 and 650 nm (604 and 655 nm when corrected for instrument response) like that of the rhenium-free analogue. However, the emission quantum yield of **[Re(CO)$_3$(Pic)Bpy-ZnTPP][OTf]** in toluene solution was reduced to 15% of the emission intensity of **Bpy-ZnTPP**, further decreasing to 6.6% in THF and 4.5% in PrCN as the solvent polarity increased.

The porphyrin fluorescence of **Bpy-MgTPP** is identical in band position and intensity to that of **MgTPP** with two intense peaks at 610 and 664 nm (612 and 665 nm corrected) in MeCN.[7] The emission spectrum of **[Re(CO)$_3$(Pic)Bpy-MgTPP][OTf]** excited at 560 nm exhibits two sharp bands at the same wavelengths as those for the rhenium-free analogue. However, the intensity in MeCN is only 2.5% of the emission intensity of **Bpy-MgTPP** (Figure 3). The excitation wavelength does not influence the relative emission yield.

No evidence of the broad featureless rhenium MLCT emission could be detected in any of the above experiments.[48] Excitation spectra also show features characteristic of the metalloporphyrins only. Strikingly, at 77 K in a methanol−ethanol (4/5 v/v) glass, the rhenium-appended porphyrin emits with similar intensity to that of the rhenium-free analogue (72% at 560 nm excitation and 92% at 600 nm excitation). Such dependence of quenching behavior on the medium is characteristic of electron-transfer processes (see Discussion).

Time-resolved Spectra. Picosecond and Nanosecond Visible Absorption Spectroscopy. Time-resolved visible absorption (TRVIS) spectroscopy was used to determine the spectra and lifetimes of transient excited states and intermediates. The transient lifetimes of the rhenium-appended porphyrins are reduced dramatically compared to their rhenium-free counterparts, but their spectra are identical.

The picosecond TRVIS spectrum of **Bpy-ZnTPP** in **PrCN** excited at 560 nm (Figure 4a) is very similar to those of **ZnTPP** and **MgTPP**[7,87] with the typical zinc porphyrin S_1 features of a strong broad absorption at 460 nm and stimulated emission at 610 and 660 nm. The transient decays negligibly on the time scale of hundreds of picoseconds.

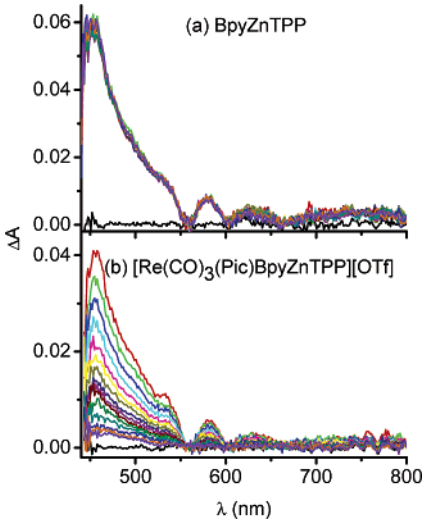

Figure 4. Ultrafast TRVIS spectra excited at 560 nm. Spectra recorded at −0.2, 1 ps, then every 4 ps to 41 ps, then 48, 58, 68, and 78 ps. (a) **Bpy-ZnTPP** in PrCN, (b) **[Re(CO)$_3$(Pic)Bpy-ZnTPP][OTf]** in PrCN.

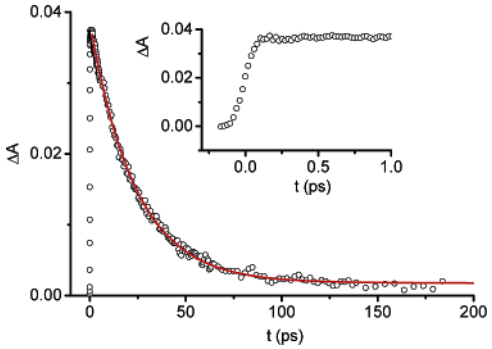

Figure 5. Decay of the TRVIS transient monitored at 463 nm following excitation of **[Re(CO)$_3$(Pic)Bpy-ZnTPP][OTf]** at 560 nm. Circles, experimental points; line, single-exponential fit. The inset shows an expansion for the first picosecond.

The TRVIS spectra of **[Re(CO)$_3$(Pic)Bpy-MTPP][OTf]** (M = Mg, Zn) in PrCN strongly resemble those of **Bpy-MTPP** with a broad absorption at 460 nm and stimulated emission at 610 nm (Figure 4b). In stark contrast to the rhenium-free metalloporphyrins, the transient species derived from **[Re(CO)$_3$(Pic)Bpy-MTPP][OTf]** in PrCN decay with lifetimes of 23.7 ± 0.2 ps (M = Zn) and 16.7 ± 0.7 ps (M = Mg) leaving very small residual absorption (Figure 4b and Figure 5). The signal rises within 200 fs (see Figure 5 inset) and decays obeying good first-order kinetics. The transient kinetics are strongly solvent dependent, with faster decay in PrCN than in THF (Table 3). The rate of decay of the transient from **[Re(CO)$_3$(Pic)Bpy-MgTPP][OTf]** is more than 2 orders of magnitude greater than that of **Bpy-MgTPP**.

It is difficult to distinguish the spectrum of the S_1 excited state from that of the porphyrin radical cation in the region 450−650 nm. However, radical cations of simple porphyrins exhibit a characteristic feature at about 700 nm.[21,88−90] We observed no bands in the region from 650 to 800 nm for **Bpy-MTPP** (M = Mg, Zn) or for their rhenium complexes.[91] The Bpy radical anion also absorbs weakly in the 650−800 nm region but was not detected.[92,93]

Table 3. Observed Lifetimes (τ) Determined by Fitting the TRVIS Decay to a Single Exponential Function

complex	solvent	τ/ps
[Re(CO)$_3$(Pic)Bpy-ZnTPP]$^+$	THF	53 ± 3
[Re(CO)$_3$(Pic)Bpy-ZnTPP]$^+$	PrCN	23.7 ± 0.2
[Re(CO)$_3$(Pic)Bpy-MgTPP]$^+$	PrCN	16.7 ± 0.7

Nanosecond time-resolved spectroscopy of zinc porphyrins probes the first triplet state, T_1. As expected, this T_1 state was detected as an intense transient on excitation of **Bpy-ZnTPP** in THF solution (excitation wavelength 532 nm, monitoring wavelength 470 nm). In a corresponding experiment with **[Re(CO)$_3$(Pic)Bpy-ZnTPP][OTf]**, the transient had only 6% of the intensity observed with **Bpy-ZnTPP** and a much longer lifetime. The reduced yield accords with the steady-state emission and the picosecond absorption experiments. The increased lifetime may be associated with a reduction in the rate of triplet−triplet annihilation because of the low concentration of triplet.

Picosecond Time-Resolved Infrared Spectroscopy. Transient visible absorption spectroscopy is only suited to study the porphyrin part of the molecule due to the strong excited-state absorption. Moreover, the S_1 state absorption spectrum consists of broad bands that are very similar to the absorption spectra of both the T_1 state and the radical cation, making it difficult to distinguish a charge-separated state from singlet or triplet states. Our compounds are designed to provide a spectroscopic handle in the infrared through CO-stretching frequencies. Consequently, picosecond time-resolved infrared (TRIR) spectroscopy should be an ideal tool for probing charge or energy transfer.

The TRIR spectrum of **[Re(CO)$_3$(Pic)Bpy-MgTPP][OTf]** in MeCN was obtained by excitation into the Q-bands of the porphyrin at 600 nm. It is characterized by two negative absorption bands (bleaches), one sharp at 2033 cm^{-1} and one broad at ∼1931 cm^{-1}, due to depletion of the ground state (Figure 6). Importantly, the negative absorption bands are present immediately after excitation, i.e., formed on a subpicosecond time scale. (They are at a maximum intensity already in the first spectrum, delay of 1.5 ps.) The bleach recovers completely with a lifetime of 34 ± 4 ps (measured at 1928 cm^{-1}, errors as 95% confidence limits, Figure 7a). In the spectrum measured after a 1.5 ps delay, there are product bands (labeled CS for charge-separated state; see Discussion) at 2008 and 1900 cm^{-1} and a positive shoulder overlapping the bleach at ca. 2028 cm^{-1}. The CS bands lie close to the positions of the one-electron reduced species detected by IR spectroelectrochemistry. The features labeled CS are at their maximum on the initial spectrum at 1.5 ps. They decay with a lifetime of 20 ± 2 ps (measured at 1893 cm^{-1}, Figure 7b) revealing after ca. 6 ps a pair of bands (labeled HG for hot ground state; see Discussion) at 2023 and 1908 cm^{-1}. The decay of this pair was fitted to a single exponential function with a lifetime of approximately 35 ± 8 ps (measured at 2023 cm^{-1}, Figure 7c) that is identical within

(85) Matousek, P.; Towrie, M.; Ma, C.; Kwok, W. M.; Phillips, D.; Toner, W. T.; Parker, A. W. *J. Raman Spectrosc.* **2001**, *32*, 983−988.
(86) Liard, D. J.; Busby, M.; Farrell, I. R.; Matousek, P.; Towrie, M.; Vlček, A., Jr. *J. Phys. Chem. A* **2004**, *108*, 2363−2369.
(87) Rodriguez, J.; Kirmaier, C.; Holten, D. *J. Am. Chem. Soc.* **1989**, *111*, 6500−6506.
(88) Kadish, K. M.; Shiue, L. R.; Rhodes, R. K.; Bottomley, L. A. *Inorg. Chem.* **1981**, *20*, 1274−1277.
(89) Kadish, K. M.; Rhodes, R. K. *Inorg. Chem.* **1981**, *20*, 2961−2966.
(90) Kadish, K. M.; Shiue, L. R. *Inorg. Chem.* **1982**, *21*, 3623−3630.
(91) TRVIS spectra of **[Re(CO)$_3$(Br)Bpy-ZnTPP]** excited at 400 nm show transient absorption in the 650−750 nm region contrasting with **[Re(CO)$_3$(Pic)Bpy-ZnTPP][OTf]**.
(92) Krejčik, M.; Vlček, A. A. *J. Electroanal. Chem.* **1991**, *313*, 243−257.
(93) Noble, B. C.; Peacock, R. D. *Spectrochimica Acta* **1990**, *46A*, 407−412.

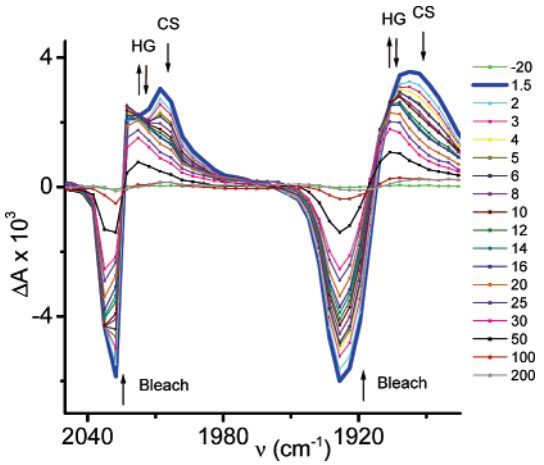

Figure 6. TRIR spectra of **[Re(CO)$_3$(Pic)Bpy-MgTPP][OTf]** in MeCN observed following 600 nm excitation. Time delays are displayed in picoseconds, the thick line is at 1.5 ps. Arrows indicate rise and decay of the transients. A function has been subtracted from all spectra, corresponding to the baseline drift measured at 2046 cm^{-1} where there is no significant absorption. The experimental points are separated by 4−5 cm^{-1}.

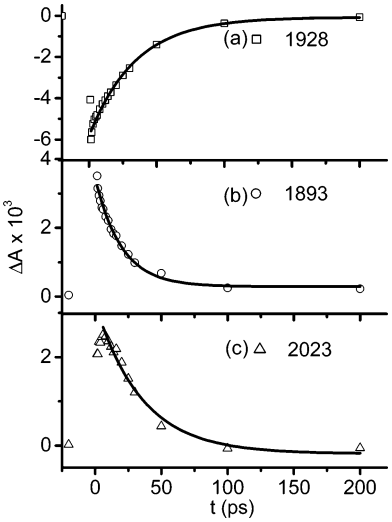

Figure 7. Transient kinetics observed by IR spectroscopy following 600 nm excitation of **[Re(CO)$_3$(Pic)Bpy-MgTPP][OTf]** in MeCN (a) bleach recovery at 1928 cm^{-1}, (b) decay at 1893 cm^{-1}, (c) decay at 2023 cm^{-1}. The lines show single-exponential fits to the experimental points shown.

Table 4. Lifetimes of Transients Observed for **[Re(CO)$_3$(Pic)Bpy-MgTPP][OTf]** in MeCN (CS Charge-Separated State, HG = Hot Ground State, 95% Confidence Limits on Last Digit in Brackets)

	TRVIS λ/nm	TRIR ν/cm^{-1}					
method	transient decay	bleach recovery	bleach recovery	CS decay	CS decay	HG decay	HG decay
probe	469	1928	2032	1893	2008	1906	2023
τ/ps	16.7 (7)	34 (4)	37(4)	20(2)	21(4)	43(8)	35(8)

experimental error to that of the bleach recovery. Lifetime data are collected in Table 4.[94] The first product state (CS) shows considerable shifts to lower frequency compared to the starting material, consistent with charge transfer from porphyrin to rhenium bipyridine (see below).

(94) Figure 5 shows a small positive spike at 2028 cm^{-1} that overlaps with the high-frequency bleach of the parent molecule. This feature may represent the $\pi\pi^*$ state that precedes formation of the CS state as is observed for **[Re(CO)$_3$(Pic)Bpy-ZnTPP][OTf]**. However, there are too few data points to be sure that it is significant. The spike is present for the first 6 ps.

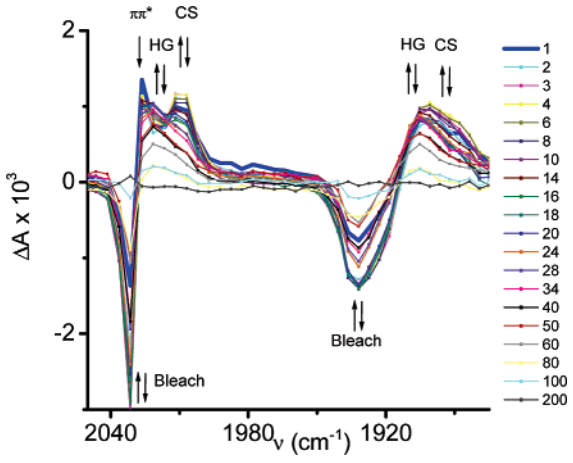

Figure 8. TRIR spectra of **[Re(CO)$_3$(Pic)Bpy-ZnTPP][OTf]** in PrCN following excitation at 560 nm. Time intervals are displayed in ps; the thick line is at 1 ps. Arrows indicate the rise and decay of the transients. A function has been subtracted from all spectra, corresponding to the baseline drift measured at 2046 cm^{-1} where there is no significant absorption. Experimental points are separated by 4−5 cm^{-1}.

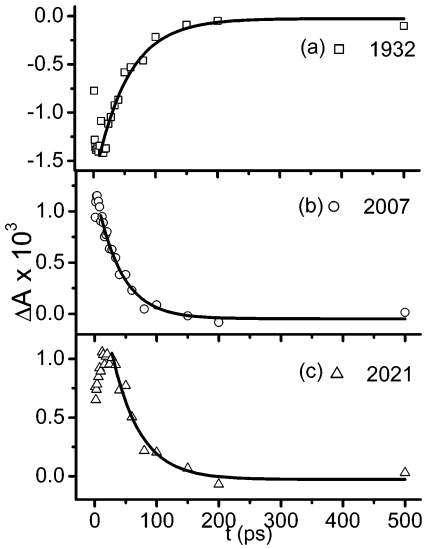

Figure 9. TRIR kinetics of **[Re(CO)$_3$(Pic)Bpy-ZnTPP][OTf]** in PrCN following 560 nm excitation. (a) Bleach at 1932 cm^{-1}, (b) CS state at 2007 cm^{-1}, (c) HG state at 2021 cm^{-1}. The lines show single-exponential fits to the points shown.

The TRIR spectrum of **[Re(CO)$_3$(Pic)Bpy-MgTPP][OTf]** was also recorded in PrCN; the more viscous solvent did not affect the spectral shape or decay kinetics of the transient significantly. Furthermore, the transient IR spectrum was recorded with both 560 and 600 nm excitation corresponding to the $Q_{0,0}$ and $Q_{0,1}$ transition in order to investigate the role of excess vibrational energy of the excited state. The decay kinetics and spectral shapes were found to be identical.

The TRIR spectra of **[Re(CO)$_3$(Pic)Bpy-ZnTPP][OTf]** in PrCN show a bleach at 2031 and 1932 cm^{-1} formed within 1 ps of excitation (the first spectrum after the laser flash) that grows to reach its maximum at about 10 ps and then decays with an average lifetime of 55 ± 8 ps (Figures 8 and 9). A product spike, labeled $\pi\pi^*$, is observed at 2026 cm^{-1} on the lower energy side of the bleach immediately after excitation (2 ps); the low-frequency partner of this band is expected to contribute to the broad maximum at 1906 cm^{-1}. These bands decay within 10 ps while a new band appears at 2007 cm^{-1}

Table 5. Lifetimes of Transients Observed for **[Re(CO)$_3$(Pic)Bpy-ZnTPP][OTf]** in MeCN (CS Charge-Separated State, HG = Hot Ground State, 95% Confidence Limits on Last Digit in Brackets)

	TRVIS λ/ nm	TRIR ν/cm^{-1}				
method	transient decay	bleach recovery	bleach recovery	$\pi\pi^*$ decay	CS decay	HG decay
probe	463	2031	1932	2026	2007	2021
τ/ps	23.7 (2)	58 (7)	52 (9)	ca. 5	40 (4)	45 (8)

and the low-frequency maximum shifts to ~1896 cm^{-1}. The new bands, labeled CS, reach their maximum at about 10 ps. The decay constant of the band at 2007 cm^{-1} is 40 ± 4 ps. Product CS gives way to a third product species by 40 ps after excitation with maxima shifted to 2021 and 1905 cm^{-1}; the decay of this product, labeled HG, is nearly complete at 100 ps. Transient kinetics are collected in Table 5.

Discussion

Ground-State Spectroscopy, Emission Quenching Mechanism, and Energetics of Electron Transfer. The rhenium-appended metalloporphyrin complexes **[Re(CO)$_3$(Pic)Bpy-MTPP][OTf]** (M = Zn, Mg) exhibit ground-state IR and UV/vis absorption spectra characteristic of the rhenium carbonyl moiety and the metalloporphyrin moiety, respectively. No new transition unique to the assembly is detectable, even at wavelengths exceeding 500 nm where the spectrum is not congested. The photophysical measurements were conducted in nitrile solvents which dissolve the compounds very well. We anticipate that the nitrile coordinates to the zinc and magnesium in the axial positions to form five- or six-coordinated metalloporphyrins. The coordination prevents aggregation at the concentrations that are used in the photophysical experiments. The emission spectra of **[Re(CO)$_3$(Pic)Bpy-MTPP][OTf]** show the two characteristic porphyrin bands at about 600 nm, but their intensities are reduced drastically (by >95% in polar solvents) relative to the bipyridine-appended porphyrins **Bpy-MTPP**. For cationic rhenium bipyridine complexes, a broad MLCT emission band is normally observed at ca. 550 nm,[48] but no such emission could be detected for **[Re(CO)$_3$(Pic)Bpy-MTPP][OTf]**.

Although the steady-state emission spectra showed no contribution assigned to the rhenium bipyridine subunit, it was evident that the presence of rhenium affects the fluorescence intensity and therefore the lifetime of the first excited singlet state, S_1 significantly. For supramolecular assemblies involving porphyrins, emission quenching is usually ascribed to energy transfer or electron transfer.[1,7] Given the strong spin−orbit coupling of the rhenium atom, enhanced intersystem crossing must also be considered as a possible reason for the reduction in emission intensity. Since the emission of the porphyrin lies to long wavelengths of the emission of related cationic rhenium complexes, energy transfer would be an endergonic process and can be ruled out. The heavy atom effect that might lead to a reduction in lifetime via spin−orbit coupling can also be excluded since the free-base analogue **[Re(CO)$_3$(Pic)Bpy-H$_2$TPP][OTf]** showed negligible emission quenching.[95]

To analyze the possibility of photoinduced electron transfer, it is essential to consider the energetics of electron transfer. An estimate of the free energy change of electron transfer can be obtained from the porphyrin emission energy in combination with the electrochemical data. Equations 1 and 2 describe the free energy expressions for oxidative and reductive electron transfer, respectively.[96] The correction term for Coulombic charge stabilization is omitted because the charge distribution is not well defined. Equation 1a shows the charge-transfer process from metalloporphyrin to rhenium bipyridine. The corresponding free energy is shown in eq 1b, where E°_{ox}(MTPP) and E°_{red}(ReBpy) are the standard potentials for oxidation of the donor (metalloporphyrin) and reduction of the acceptor (rhenium bipyridine) and F is the Faraday; E^*_{00} is the emission energy of the porphyrin in eV which approximates to the energy of its excited state.

$$*\mathbf{[Re^{+}(CO)_3(Pic)Bpy\text{-}MTPP]} \rightarrow \mathbf{[Re^{+}(CO)_3(Pic)Bpy^{-\bullet}\text{-}MTPP^{+\bullet}]} \quad (1a)$$

$$\Delta G^\circ_{ox} = FE^\circ_{ox}(\mathrm{MTPP}) - FE^\circ_{red}(\mathrm{ReBpy}) - E^*_{00} \quad (1b)$$

Equation 2a shows the charge-transfer process from rhenium bipyridine to metalloporphyrin. The corresponding free energy is shown in eq 2b, where E°_{ox}(ReBpy) and E°_{red}(MTPP) are the standard potentials for oxidation of the donor (rhenium bipyridine) and reduction of the acceptor (metalloporphyrin); E^*_{00} is unchanged.

$$*\mathbf{[Re^{+}(CO)_3(Pic)Bpy\text{-}MTPP]} \rightarrow \mathbf{[Re^{2+}(CO)_3(Pic)Bpy\text{-}MTPP^{-\bullet}]} \quad (2a)$$

$$\Delta G^\circ_{red} = FE^\circ_{red}(\mathit{MTPP}) - FE^\circ_{ox}(\mathrm{Re}\mathit{Bpy}) + E^*_{00} \quad (2b)$$

We use the data in Table 2 for **[Re(CO)$_3$(Pic)Bpy-ZnTPP][OTf]**. Table 6 shows oxidation potentials and low-temperature emission data for **Bpy-ZnTPP** and **Bpy-MgTPP** together with the derived excited-state oxidation potential. For the rhenium moiety, we employed [Re(CO)$_3$(Pic)(bpy)]$^+$ as a model which has an oxidation potential of 1.41 V.[97]

We consider four processes: (a) oxidative quenching of the S_1 state by electron transfer from the porphyrin to the Re(bpy) moiety; (b) reductive quenching from Re(bpy) to the porphyrin S_1 state; (c) oxidative quenching from the porphyrin T_1 state to Re(bpy); (d) reductive quenching from the porphyrin T_1 state to Re(bpy). Processes b, c, and d may be excluded since they are calculated to be strongly endergonic. For instance, ΔG° is calculated as +1.2 eV for process b in both **[Re(CO)$_3$(Pic)Bpy-MgTPP][OTf]** and its zinc analogue. In contrast, process a is calculated to be an exergonic process with $\Delta G^\circ = -0.32$

Table 6. Electrochemical Data in THF vs Fc/Fc$^+$, Low Temperature Emission Data in MeOH/EtOH 4/5 Glass at 77 K,[a] and Derived Excited State Oxidation Potential for **Bpy-MTPP**

porphyrin	E_{ox}/V	$E^*_{00}(S_1)$/eV	E^*_{ox}/V[b]
Bpy-ZnTPP	0.38	2.06	−1.68
Bpy-MgTPP	0.24	2.00	−1.76

[a] We use measurements made at 77 K in order to minimize the effect of thermal excitation,[7] although the differences from the room-temperature measurements are negligible. [b] E^*_{ox} is given by $E_{ox} - E^*_{00}$.

(95) Gabrielsson, A. Ph.D. Thesis, University of York, York, U.K., 2002.

(96) Rehm, D.; Weller, A. *Isr. J. Chem* **1970**, *8*, 259−271.

(97) Sacksteder, L.; Zipp, A. P.; Brown, E. A.; Streich, J.; Demas, J. N.; Degraff, B. A. *Inorg. Chem.* **1990**, *29*, 4335−4340.

eV for **[Re(CO)$_3$(Pic)Bpy-MgTPP][OTf]** and −0.24 eV for its Zn analogue. Since, the chemical irreversibility of the reduction process makes an accurate measurement of the reduction potential impossible, these values should be considered approximate. In conclusion, energetic arguments support electron transfer from metalloporphyrin to rhenium bipyridine as the most likely quenching mechanism. The reduced quenching in a low temperature glass also suggests an electron transfer mechanism since electron transfer processes are usually suppressed in rigid media.

Picosecond Spectroscopy and Photochemical Mechanism. Transient Visible Absorption Spectra. The picosecond TRVIS spectra of **Bpy-MgTPP** and **Bpy-ZnTPP** show typical magnesium porphyrin S_1 features. In PrCN, the S_1 excited states of **Bpy-MTPP** (M = Mg, Zn) decay on a longer time scale than the instrument is capable of measuring. It is reasonable to assume that the lifetime of **Bpy-MTPP** is similar to that of **MTPP**, viz. ca. 3 ns in polar solvents.[7]

The presence of the rhenium moiety in **[Re(CO)$_3$(Pic)Bpy-MTPP][OTf]** affects the porphyrin TRVIS kinetics drastically, and the lifetime of the transient is reduced to 23.7 ± 0.2 and 16.7 ± 0.7 ps for M = Zn and Mg, respectively (PrCN solvent). The transient spectrum is affected very little by the rhenium moiety, and product bands at very long wavelengths characteristic of a radical cation are absent. If the spectrum arises from a CS state rather than an S_1 state, there should also be changes in the absorption coefficient (and hence intensity) in the 470-nm region. We employ the absorption coefficients to obtain additional evidence to distinguish whether the signal arises from the S_1 or the CS species. The change upon excitation in the molar absorption coefficient, $\Delta\epsilon$, in the S_1 state of **ZnTPP** has been estimated as ca. 7.1×10^4 dm^3 mol^{-1} s^{-1} at 470 nm.[98] The corresponding value for the oxidation of **Bpy-ZnTPP** was estimated from our spectroelectrochemical data to lie in the range $\Delta\epsilon = 1.8 \times 10^4$ to 3.4×10^4 dm^3 mol^{-1} s^{-1} (see above). The maximum value is about half that of the S_1 state. The spectroelectrochemical data also show that $\Delta\epsilon$ at 650 nm is ca. 60% of $\Delta\epsilon$ at 470 nm. When we compare the picosecond spectra of **Bpy-ZnTPP** and **[Re(CO)$_3$(Pic)Bpy-MTPP][OTf]**, we see a loss of ca. 30% in intensity but no change in band shape. If the charge-shifted state were the only species present on irradiation of **[Re(CO)$_3$(Pic)Bpy-MTPP][OTf]**, the reduction in intensity should be far greater and the cation features in the region 650−750 nm should be detectable. We infer from these considerations that the ultrafast visible spectra are dominated by excited state(s) of **[Re(CO)$_3$(Pic)Bpy-MTPP][OTf]** of S_1-($\pi\pi^*$) type.

Transient IR Spectra. Transient IR spectra of Re(CO)$_3$(bpy) complexes typically show a shift of the ν(CO) bands to high frequency because of population of the MLCT excited state[68,73,74,99,100] that creates a positive charge at the metal center, reducing the Re-to-CO π-back-bonding and increasing ν(CO). Intraligand excitation is expected to result in only small negative shifts in ν(CO). For instance, Dattelbaum et al.[73] have observed shifts of −5 and −10 cm^{-1} for [Re(CO)$_3$(4-Et-py)(Me$_2$-dppz)]$^+$ (dppz = dipyridophenazine). Comparable shifts were observed in other examples such as [Re(CO)$_3$(PPh$_3$)(dppz)]$^+$ (average shift −8 cm^{-1}), [Re(CO)$_3$(4-styrylpyridine)(bpy)]$^+$ (shift −7 cm^{-1}), and [Re(CO)$_3$(py)(11,12-dichloro-dppz)]$^+$ (shifts −8 and −14 cm^{-1}).[67,72,101,102] In contrast, electron transfer from the metalloporphyrin to Re(CO)$_3$(bpy) would be expected to cause a low-frequency shift characteristic of increased Re-to-CO π-back-bonding. TRIR spectra of such reduced photoproducts are expected to be similar to IR spectra of electrochemically generated [Re(CO)$_3$(L)(bpy$^{\bullet-}$)] complexes.[63−65]

A. TRIR Spectra of Magnesium Porphyrin. Picosecond transient infrared spectroscopy of **[Re(CO)$_3$(Pic)Bpy-MgTPP][OTf]** in MeCN provides an unequivocal demonstration of an ultrafast charge transfer, since (a) the maximum bleach is detected at the first measurement after the flash (1.5 ps) and (b) the product ν(CO) bands lie considerably to low wavenumbers of the precursor. It should be stressed that the rhenium moiety does not absorb at the excitation wavelengths (560 or 600 nm) and therefore Re(bpy) excited states cannot be populated directly. Likewise, two-photon absorption was excluded by attenuating the excitation power. The signal intensity was found to decrease linearly with the pump energy, rather than the square of pump energy as would be expected for two-photon absorption.

The product bands labeled CS are shifted to lower frequency with respect to the precursor and decay with a lifetime of 20 ± 2 ps. The shifts are −24 cm^{-1} for the high-frequency band and −35 cm^{-1} for the low-frequency band. To test whether the CS state contains a reduced **[Re$^+$(CO)$_3$(Pic)Bpy$^{\bullet-}$]** unit, we compare the TRIR spectra with the spectrum of electrochemically generated **[Re(CO)$_3$(Pic)Bpy-ZnTPP]**. For quantitative comparison, the shift between the cation and radical forms of electrochemically reduced **[Re(CO)$_3$(Pic)Bpy-ZnTPP][OTf]** is −23 cm^{-1} for the high frequency and −31 cm^{-1} for the low-frequency band. Thus the bands labeled as CS are consistent with a charge-separated excited state in which the Re(bpy) unit has been converted from cation to radical and the Mg(TPP) from neutral to radical cation, **[Re$^+$(CO)$_3$(Pic)Bpy$^{\bullet-}$-MgTPP$^{\bullet+}$]**. The spectroelectrochemical data were used to estimate that the absorption coefficient of the high frequency band of the radical anion is about 57% that of the parent. If the same applies to the CS state, we can compare the intensities of the high frequency bands of the bleach and the CS state at early times in order to estimate the proportion of the product in the CS state. This method indicates that at least half the product detected by TRIR spectroscopy is in the CS state at the early times.

The description of the product state as charge-separated (CS) represents a simplification that neglects the coupling between the components of the molecule. Alternative descriptors are redox-separated (RS)[73] or a shift of positive charge from the Re(bpy) unit to the metalloporphyrin unit. The minimum distance between donor and acceptor centers may be taken as the edge-to-edge separation of the porphyrin and bpy units, which is seven CC or CN bonds.

Further interpretation is assisted by combining the information from TRIR and TRVIS spectra. The TRVIS spectra decay (τ = 16.7 ± 0.7 ps) at a rate that is close to the decay rate of CS bands (τ = 20 ± 2 ps) but faster than the bleach recovery in the TRIR spectra ($\tau \approx$ 35 ps). However, a further product (HG)

(98) Harriman, A. *J. Chem. Soc., Faraday Trans. 2* **1981**, *77*, 1281−1291.
(99) Dattelbaum, D. M.; Meyer, T. J. *J. Phys. Chem. A* **2002**, *106*, 4519−4524.
(100) Dattelbaum, D. M.; Omberg, K. M.; Schoonover, J. R.; Martin, R. L.; Meyer, T. J. *Inorg. Chem.* **2002**, *41*, 6071−6079.
(101) Schoonover, J. R.; Strouse, G. F.; Dyer, R. B.; Bates, W. D.; Chen, P. Y.; Meyer, T. J. *Inorg. Chem.* **1996**, *35*, 273−274.
(102) Busby, M.; Matousek, P.; Towrie, M.; Vlček, A. *J. Phys. Chem. A* **2005**, *109*, 3000−3008.

is observed in the TRIR spectra that decays with a lifetime of ca. 39 ps. This species has no counterpart in the TRVIS spectra, suggesting that it does not correspond to an electronically excited state. It is not possible to obtain accurate decay kinetics for the HG state from the TRIR spectra because the bands of the two products overlap, but the lifetime of HG is similar to that of the bleach recovery. The HG state has broad bands that are still shifted to low wavenumbers but are considerably closer to those of the ground state. The kinetic and spectroscopic evidence strongly suggests that the HG state is the intermediate between the CS state and the bleach recovery. It is assigned to a Hot Ground state, i.e., a vibrationally excited state.

B. TRIR Spectra of Zinc Porphyrin. The behavior of the Zn complex, **[Re(CO)$_3$(Pic)Bpy-ZnTPP][OTf]**, is qualitatively the same as that of the magnesium complex but *quantitatively* different. In the TRIR spectra, a spike that overlaps with the high frequency bleach of the parent is observed for the first five picoseconds (Figure 8). It is provisionally assigned as an initial excited state, $\pi\pi^*$, of the parent but may represent only a reactive conformer of this state (see below). The bleach and the CS state reach a maximum only after 5 ps. The kinetics of the CS state could not be obtained as accurately as for the magnesium complex because the problem of overlap with the HG state was more severe. The slower rise of the CS state may be associated with the reduced free energy of charge separation for the zinc complex.

Mechanistic Conclusions. The conclusions from this analysis can be summarized as follows. (a) The transient UV/vis spectra are dominated by excited states of S_1 ($\pi\pi^*$) type, but the clean first-order kinetics belie considerable complexity that is revealed by the transient IR spectra. (b) The transient IR spectra inform us that there is a substantial proportion of CS state from the earliest time delays measured. The CS state is at its maximum for the magnesium complex with a delay of 1 ps, while the CS state maximizes at ca. 5 ps for the zinc complex. (c) The CS state decays initially to vibrationally excited levels of the electronic ground state. (d) The deductions from the TRVIS spectra can be reconciled with the TRIR data if there is branching between two pathways, such that there are substantial proportions of both the S_1 state and the CS state populated within 1 (M = Mg) or 5 (M = Zn) ps. The latter accounts for at least 50% of promptly formed photoproducts. The photochemical observations derived above for **[Re(CO)$_3$(Pic)Bpy-MTPP][OTf]** (M = Mg, Zn) are summarized in Scheme 2.

We have considered several kinetic models that could account for the data. The most satisfactory model (*multiple conformations*) postulates that the rates of forward and back electron-transfer vary with the torsional angles between the porphyrin plane and the C_6H_4 plane and that several conformers with different torsional angles are present; twisted conformations will be more populated, but there is restricted overlap between the bridge and the porphyrin π-system that reduces the rate of electron transfer when compared to conformers that are close to coplanar. Optical excitation of the reactive (coplanar) conformer A yields the excited-state A* which is responsible for the subpicosecond formation of the CS state (Scheme 3). The apparent rate constant of the S_1 decay corresponds to the combination of the rate constants of conformational changes and/or of charge separation in less favorable conformations B*, C*,... of the excited state. Similarly, the apparent rate constant

Scheme 2. Photochemical Pathways for **[Re(CO)$_3$(Pic)Bpy-MTPP][OTf]** (lifetimes M = Mg, red; M= Zn, black)[a]

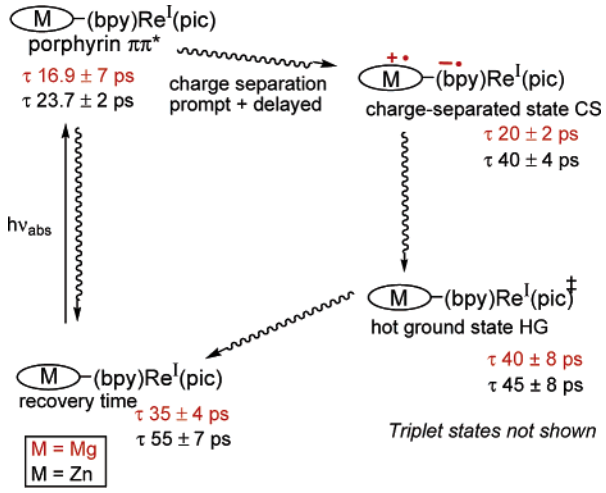

[a] The times indicate measured lifetimes with 95% confidence limits.

for the decay of the CS state may correspond to the combination of rate constants for back-electron transfer of different conformers. Rate constants for back electron transfer for individual conformers may be appreciably faster than the measured rate constant. Detailed kinetic modeling will await studies on related systems.

In an alternative model (*fast back electron transfer*) it is postulated that the kinetics observed by transient visible spectroscopy correspond to the charge-separation process, but the back electron transfer to HG is considerably faster. Simulation of this model indicates that the concentration of the CS state would be no more than 5% of the S_1 state, if the CS state is to reach its peak 1 ps after the flash (M = Mg) or 5 ps after the flash (M = Zn). This figure is inconsistent with the estimate above that the proportion of CS state contributing at early times corresponds to at least 50% of the bleach of the TRIR spectrum. Since, we could only reconcile this model with the data if a large proportion of the molecules in the excited state make no contribution to the TRIR spectrum, we favor the multiple conformation model. Two other models are summarized in the footnotes.[103]

Therien et al. have studied the formation of charge-separated states of zinc porphyrins linked to quinones in supramolecular assemblies by both transient absorption and transient IR spectroscopy with subpicosecond time resolution. They have observed that charge separation occurs in the time range of 20 fs to 3 ps according to the donor−acceptor distance.[20−22] They have also used TRIR spectroscopy to monitor variations in the mixing of the donor and acceptor states. Therien et al. also

(103) We have also considered two further models. (a) *Ultrafast Equilibrium*: excitation leads to an ultrafast equilibrium between the CS and S_1 states, implying that the CS and S_1 states are much closer in energy than the electrochemical calculations indicate. (b) *Delocalized CS State*: the CS state branches from the S_1 precursor state on a subpicosecond time scale for M = Mg and 5 ps time scale for M = Zn and is the major species during the first 5 ps; it decays in 20 ps (Mg) or 40 s (Zn) by back electron transfer. This model also requires a channel for conversion of the residual S_1 state into CS either by the conformational mechanism or by an ultrafast equilibrium. It differs from these mechanisms in containing an additional postulate, namely that the UV/vis spectrum of the CS state resembles that of the S_1 state because it is highly delocalized at least in its own upper state. As a result the contributions to the TRVIS spectrum from CS and the S_1 state resemble one another. This idea chimes with Therien's proposal for enhanced delocalization of the CS state compared to the S_1 state.[104]

Scheme 3. Model for Formation of CS State from Several Conformers of Parent Complex; the Observed Kinetic Behavior Corresponds to the Sum of the Contributions from the Various Conformers

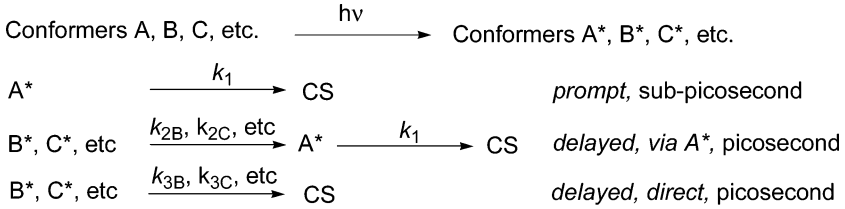

studied porphyrins linked to diimines via an ethynyl bridge and proposed that charge recombination is faster than forward electron transfer.[104] This analysis includes a demonstration that different conformations have a small effect on the energetics of electron transfer. One of the closest examples to **[Re(CO)$_3$(Pic)Bpy-MTPP][OTf]** reports photophysical data for zinc and magnesium porphyrins linked via an ethynyl bridge to square planar platinum centers.[33] As in our own examples, these complexes show extensive quenching of the porphyrin-based excited state but no sign of the signature of the radical cation in the TRVIS spectrum. The authors suggest that back electron transfer is faster than forward electron transfer but do not have the benefit of TRIR spectroscopy to test their proposal.

Back-Electron Transfer and Formation of the Hot Ground State. We conclude above that back electron-transfer results in formation of a hot ground (HG) state prior to return to the initial state. Here we set this hypothesis in context. Photodissociation of metal carbonyls can result in initial formation of metal carbonyl intermediates in their ground electronic state but excited vibrational states. Two distinguishable situations have been observed: (a) population of the $v = 1$ ν(CO) level manifested by separate bands for the ν(CO) 0→1 and 1→2 transitions, the latter shifted by ca. −15 cm^{-1};[105] (b) excitation of low frequency vibrational modes that are anharmonically coupled to ν(CO) modes, resulting in a downshift of all ν(CO) modes. In this situation, the hot bands are not well resolved, and their population decreases as the vibrational levels relax resulting in a high-frequency shift.[106] Vibrational spectra of excited states of metal carbonyls have also revealed downshifts in ν(CO) due to population of coupled low-frequency modes similar to that summarized in (b).[102,107] In **[Re(CO)$_3$(Pic)Bpy-MTPP][OTf]**, there is sufficient excess energy to populate such hot ground states after photoinduced electron transfer, and our metal carbonyl system is well adapted to observe this effect (free energies for back-electron transfer are calculated as −1.68 and −1.76 eV for Mg and Zn, respectively; see Table 6).

The back-electron transfer in **[Re(CO)$_3$(Pic)Bpy-MTPP][OTf]** takes place in the Marcus inverted region where the driving force exceeds the reorganization energy. Theory predicts that population of higher vibrational levels, as postulated in the formation of the HG state, will speed up a reaction in the Marcus inverted region. The electron transfer populates vibrations which accept some of the excess free energy released during the reaction, effectively reducing the barriers and increasing the rate.[108−112] The spectroscopic detection of the vibrationally hot product (HG) is thus in accordance with the surprisingly fast back reaction which exceeds the rate of vibrational cooling of the ground state. We are not aware of a previous observation of a hot ground state in an electron-transfer reaction in the Marcus inverted region that could be used to test the theory.

Mechanism of Photosubstitution at Remote Site in the Presence of NEt$_3$. In this section, we demonstrate how the photoreactions that we observed previously may be reconciled with the results reported here. We showed earlier that long wavelength irradiation (λ > 450 nm) of **[Re(CO)$_3$(Pic)Bpy-ZnTPP][OTf]** in the presence of halide ions leads to replacement of coordinated picoline by halide. Photolysis in the absence of halide leads to substitution of picoline by the solvent (THF). If excess 3-picoline is added in addition to Et$_3$N, the 1e-reduced species **[Re$^+$(CO)$_3$(Pic)Bpy$^{\bullet-}$-ZnTPP]** is formed.[23] Similar observations have been made for **[Re$^+$(CO)$_3$(Pic)Bpy$^{\bullet-}$-MgTPP].**[95] The experiments reported here show that the IR bands of the CS state rise and decay in the 1−40 ps time domain. (Because of the rapid quenching of the singlet state, triplet photochemistry is not significant.) It follows that any electron transfer from triethylamine to the metalloporphyrin must be complete within the lifetime of the CS state, implying that the Et$_3$N donor must be coordinated to the Mg or Zn prior to excitation. Coordination of nitrogen to zinc porphyrins to form 5- and 6-coordinate complexes is well established.[113,114] The energetics and dynamics of coordination are also well documented.[115] Following photoinduced electron transfer from the metalloporhyrin to the rhenium bipyridine center, irreversible electron transfer from the coordinated triethylamine to the metalloporphyrin can fill the hole at the porphyrin and the oxidized triethylamine will decoordinate. This process results in a long-lived radical, **[Re$^+$(CO)$_3$(Pic)Bpy$^{\bullet-}$-MTPP]**, that is stable in the presence of excess 3-picoline but undergoes substitution of 3-picoline by halide or solvent in its absence.

Conclusions

In this paper, we have reported the synthesis and photophysics of magnesium and zinc porphyrins covalently linked via an amide bond to a rhenium(bipyridine)tricarbonyl unit. The design of the assembly allows for probing of the porphyrin moiety via absorption and emission spectroscopy and the rhenium bipyridine moiety via IR spectroscopy. The conjugated bridge and

(104) Redmore, N. P.; Rubtsov, I. V.; Therien, M. J. *J. Am. Chem. Soc.* **2003**, *125*, 8769−8778.
(105) Dougherty, T. P.; Heilweil, E. J. *J. Chem. Phys.* **1994**, *100*, 4006−4009.
(106) Lian, T. Q.; Bromberg, S. E.; Asplund, M. C.; Yang, H.; Harris, C. B. *J. Phys. Chem.* **1996**, *100*, 11994−12001.
(107) Liard, D. J.; Busby, M.; Matousek, P.; Towrie, M.; Vlček, A., Jr. *J. Phys. Chem. A* **2004**, *108*, 2363−2369.
(108) Brunschwig, B. S.; Sutin, N. *Comments Inorg. Chem.* **1987**, *6*, 209−235.
(109) Sutin, N.; Creutz, C.; Fujita, E. *Comments Inorg. Chem.* **1997**, *19*, 67−92.
(110) Jortner, J.; Bixon, M. *J. Chem. Phys.* **1988**, *88*, 167−170.
(111) Omberg, K. M.; Chen, P. Y.; Meyer, T. J. *Adv. Chem. Phys.* **1999**, *106*, 553−570.
(112) Bixon, M.; Jortner, J. *Adv. Chem. Phys.* **1999**, *106*, 35−202.
(113) Scheidt, W. R.; Lee, Y. J. *Struct. Bonding (Berlin)*, 1987; Vol. 64.
(114) Senge, M. O.; Kalisch, W. W. *Inorg. Chem.* **1997**, *36*, 6103−6116.
(115) Sanders, J. K. M.; Bampos, N.; Clyde-Watson, Z.; Darling, S. L.; Hawley, J. C.; Kim, H.-J.; Mak, C. C.; Webb, S. J. In *The Porphyrin Handbook*; Kadish, K. M., Smith, K. M., Guilard, R., Eds.; Academic Press: New York, 2000; Vol. 3.

the electron accepting properties of the **[Re$^+$(CO)$_3$(Pic)Bpy]** unit make this design well adapted for fast electron transfer. Although there is no discernible interaction between the rhenium(bipyridine)tricarbonyl and the metalloporphyrin moieties in the ground electronic state, the systems exhibit remarkable photophysical and photochemical properties.

When the assembly is excited at long wavelengths in a region where all absorption relates to the porphyrin, electron transfer from porphyrin to rhenium bipyridine occurs on an ultrafast time scale. In the case of the magnesium porphyrin, the IR bands of the charge-separated excited state are observed after 1.5 ps and decay in ca. 20 ps. For the zinc analogue, the corresponding rise takes ca. 5 ps and the decay 40 ps. The charge-separated excited state may be approximated by the description **[Re$^+$-(CO)$_3$(Pic)Bpy$^-$-MTPP$^{\bullet+}$]**. A further state is identified in the IR spectra at a stage when the transient absorption signal has disappeared. It is characterized by a reduced low-frequency shift of the ν(CO) bands and is assigned to a species that remains vibrationally excited but is in the ground electronic state. The assembly returns to its initial (vibrational and electronic ground state) with a time constant of 35−55 ps. This rapid charge separation and back electron transfer process provides a mechanism for quenching of the porphyrin emission that is solvent dependent.

The system is reversible in the absence of an added electron donor but undergoes irreversible reaction at the reduced rhenium bipyridine center in the presence of added triethylamine. The observation of productive reaction at the rhenium site on irradiation into the absorption of the metalloporphyrin site is compatible with ultrafast back electron transfer provided that (a) triethylamine coordinates to zinc or magnesium prior to absorption and (b) electron transfer from the metalloporphyrin to the bipyridine is followed rapidly by irreversible electron transfer from the triethylamine to the metalloporphyrin.

The experiments graphically demonstrate benefits of the incorporation of carbonyl ligands on the electron acceptor, since the sequence of charge separation and back electron transfer can only be identified correctly with the aid of the time-resolved IR data. They emphasize the utility of the **[Re$^+$(CO)$_3$(Pic)Bpy]** unit as an electron acceptor and the rapidity of photoinduced electron-transfer processes even in quite large and complex molecules.

Acknowledgment. We acknowledge support from COST D14 and D35, EPSRC, CCLRC, and the University of York. Furthermore, we thank Mr. Taasje Mahabiersing and Mr. Michiel Groeneveld (University of Amsterdam) for their help with the TRVIS experiments. We also acknowledge Dr. Trevor Dransfield of the University of York mass spectrometry service and the EPSRC National Mass Spectrometry Service Centre in Swansea. We appreciated the helpful comments of the referees and of Dr. John Moore.

Supporting Information Available: Synthesis of **Bpy-ZnTPP**; Table S1, ^{1}H NMR data for **Bpy-ZnTPP** and **Bpy-MgTPP**; Figures S1−S3, ^{1}H NMR spectra of **[Re(CO)$_3$(Pic)-Bpy-MTPP][OTf] (M = Mg, Zn)**; Figure S4, Electronic absorption spectra of **Bpy-MgTPP** and **[Re(CO)$_3$(Pic)Bpy-MgTPP][OTf]**. Figure S5, UV/vis spectroelectrochemistry of **Bpy-ZnTPP**. This material is available free of charge via the Internet at http://pubs.acs.org.

JA0539802